Turkish Journal of Earth Sciences

Manuscript 1944

# Kinematics and age of the Afyon Zone in the Akhisar region, western Türkiye

TALİP GÜNGÖR

İSMAİL İŞİNTEK

ERHAN AKAY

CÜNEYT AKAL

ALTUĞ HASÖZBEK

See next page for additional authors

# Kinematics and age of the Afyon Zone in the Akhisar region, western Türkiye

Authors
TALİP GÜNGÖR, İSMAİL İŞİNTEK, ERHAN AKAY, CÜNEYT AKAL, ALTUĞ HASÖZBEK, AHMED ERBİL, and AXEL GERDES

Turkish Journal of Earth Sciences

http://journals.tubitak.gov.tr/earth/

Research Article

Turkish J Earth Sci
(2025) 34: 23-46
© TÜBİTAK
doi:10.55730/1300-0985.1944

# Kinematics and age of the Afyon Zone in the Akhisar region, western Türkiye

**Talip GÜNGÖR**[1,*], **İsmail İŞİNTEK**[1], **Erhan AKAY**[1], **Cüneyt AKAL**[1], **Altuğ HASÖZBEK**[2], **Ahmed ERBİL**[3], **Axel GERDES**[4]

[1]Department of Geological Engineering, Faculty of Engineering, Dokuz Eylül University, İzmir, Turkiye
[2]National Research Center on Human Evolution: Burgos, Castilla y Leon, Spain
[3]70 Ivybridge Drive, Brampton, Ontario, Canada
[4]Department of Geosciences, Goethe University Frankfurt, Frankfurt am Main, Germany

**Received:** 20.05.2024 • **Accepted/Published Online:** 17.11.2024 • **Final Version:** 24.01.2025

**Abstract**: In western Anatolia, to the south of the İzmir–Ankara Suture, the Menderes Massif, Cycladic Blueschists, Afyon Zone, and Bornova Mélange form the main tectonic belts from bottom to top structurally. In the Akhisar region, the Akhisar Nappe consists of the Hasköy Formation below and the Görenez Limestone above. The Hasköy Formation is composed of a metaclastic sequence with metarhyolite intercalations (237.4 ± 1.1 Ma, zircon LA-ICP-MS) and recrystallized limestone lenses, and it gradually passes upward into Late Norian–Early Jurassic Görenez Limestone. New radiogenic data from metarhyolites of the Hasköy Formation and fossil determinations from recrystallized limestones of the Görenez Limestone show that the age of the Akhisar Nappe ranges from early Late Triassic to Early Jurassic. Along the contact between the Akhisar Nappe and the Menderes Massif, the linear fabric and associated asymmetric structures in the mylonitic fault zone indicate a top-NE shear sense. Correlation between the internal stratigraphy of the Akhisar Nappe and the Mesozoic part of the Afyon Zone sequences in its eastern part indicates that the Akhisar Nappe is the western continuation of the Afyon Zone.

**Key words:** Afyon Zone, U–Pb zircon ages, Triassic rhyolites, late Triassic–Early Jurassic fossils

## 1. Introduction

In western Anatolia, between the Sakarya Zone to the north and the Anatolide–Tauride Platform (Şengör and Yılmaz, 1981) to the south, various parts of these two blocks and remnants of the intervening Tethys Ocean were subjected to tectonic and metamorphic overprinting during the Alpine Orogeny to form a complex nappe pile (Ketin, 1966; Şengör and Yılmaz, 1981; Erdoğan, 1990a, 1990b; Okay and Tüysüz, 1999; Okay et al., 1990, 1996, 1998, 2002). The tectonic belts formed by closing of the Neotethys are the Tavşanlı Zone (Okay, 1986), Afyon Zone (Okay 1984), Menderes Massif (Durr et al., 1978), Cycladic Blueschists, and Lycian Nappes from north to south (Figure 1). A SW–NE-trending nonmetamorphic part of this tectonic pile, the Bornova Flysch Zone (Okay et al., 1996) including the strongly sheared, blocky Bornova Mélange (Erdoğan, 1990a, 1990b) and Karaburun Belt extends from İzmir to Balıkesir along the western edge of this collision zone (Figure 1).

The Afyon Zone of this tectonic pile was first named by Okay (1984). Authors redefined the formerly described "low-grade metamorphic uppermost part of the Menderes Massif" of Akdeniz and Konak (1979a, 1979b) and "low grade metasedimentary rocks (anchimetamorphic zone)" of Kaya (1972) and Kaya et al. (1995), as the deeply submerged, HP/LT metamorphic part of the northern margin of Anatolide–Tauride Platform and named this tectonostratigraphic zone the Afyon Zone. Later, Özcan et al. (1988) renamed the association the Kütahya–Bolkardağ Belt and described it as a Palaeozoic–Mesozoic sequence of metaclastics and carbonates that formed along the northern edge of the Anatolide–Tauride Platform. In the Kütahya–Bolkardağ Belt, four rock associations separated by unconformities are described as follows (Göncüoğlu et al., 2003): (1) Silurian–Devonian carbonate succession, (2) Carboniferous to Permian metaclastics and metavolcanics including Carboniferous limestone blocks, (3) Mesozoic clastics and carbonates overlain by Late Cretaceous ophiolites, and (4) Cenozoic cover.

In the Afyon and Konya regions and along the east and southeast edges of the Menderes Massif, Candan et al. (2005) divided the central part of the Afyon Zone into two assemblages: (1) a lower assemblage of amphibolite–facies schists with mafic–felsic metaigneous rocks (Pan-

* Correspondence: talip.gungor@deu.edu.tr

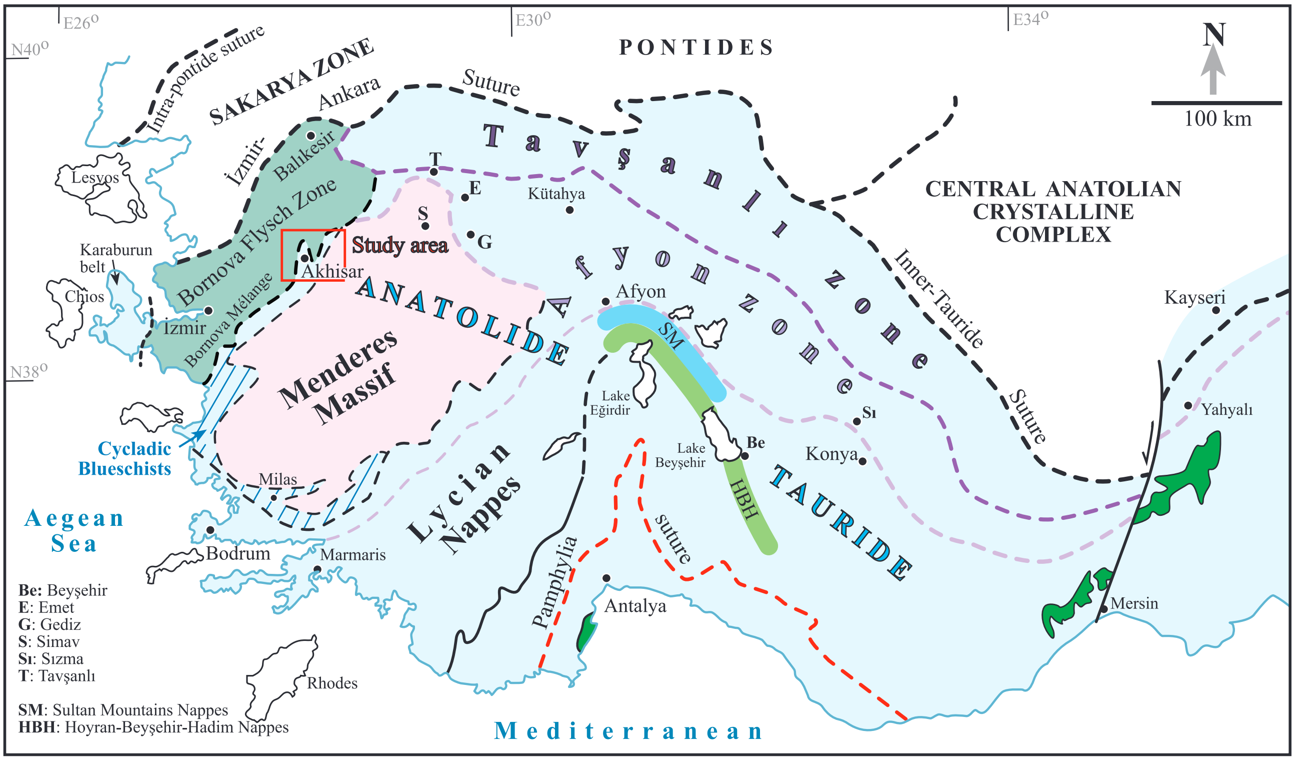


**Figure 1.** Map showing location of the study area and the main tectonic belts of southwest Türkiye to the south of the İzmir–Ankara suture (compiled following Ketin, 1966; Brunn et al., 1971; De Graciancky, 1972; Özgül, 1976; Okay and Tüysüz, 1999; Parlak and Delaloye, 1999; Okay et al., 2001; Robertson et al., 2003; Moix et al., 2008; Pourteau et al., 2010, 2013, 2016; Akay et al., 2011).

African basement), (2) an upper assemblage of low-grade metasediments including metaconglomerates, schist, phyllites, and metacarbonates.

The internal stratigraphy, geochemical characteristics of the metarhyolite intervals in the lower part, and fossil content of the carbonate succession in the upper part of the Afyon Zone around Emet (Kütahya) (Figure 1) were defined by Akay et al. (2011). Paleontological determinations, documented in the present study, reveal that the upper part of the Afyon Zone succession (Budağan Limestone) is Late Triassic to Kimmeridgian in age (Figure 2) in the Emet region. Southeastward, in the Avdan-Sızma (Konya) region, Akal et al. (2005, 2012, 2024) obtained zircon evaporation ages of 240.8 ± 3.7 Ma and 250.1 ± 3.8 Ma from the metarhyolites and metatrachyandesites in the metasedimentary lower part of the Afyon Zone.

In most of the previous studies, along the west and northwest borders of the Menderes Massif, from Balıkesir to further southwest to İzmir (Figure 1), the extension of the Afyon Zone is indistinct along the northern flank of the Tauride–Anatolide Block. Along a narrow belt from İzmir to Akhisar and further northeast to Simav, mapping of the Afyon Zone is unclear on top of the Menderes Massif. A regional map published by Göncüoğlu (1997) shows the westward continuation of the Kütahya–Bolkardağ Belt along the northwest edge of the Menderes Massif up to the Karaburun Belt. However, this map is not supported by local observations, proper mappings, or descriptions of the exposures of the Afyon Zone in these localities. Lately, contrary to the earlier studies, Pourteau et al. (2013) suggested a new paleogeographic–paleotectonic reconstruction and claimed that the Afyon Zone tectonically covers the northern, eastern, and southern flanks of the Menderes Massif and Cycladic Blueschists (Figure 1).

In western Anatolia, around Akhisar, a Mesozoic sequence composed of metaclastic rocks in the lower part and recrystallized carbonates in the upper part crops out. Akdeniz et al. (1980) divided this sequence into two units: (1) the Jurassic Hasköy Formation consisting of red metaclastics with metarhyolites in the lower part, (2) the Jurassic–Cretaceous Görenez Limestone consisting of recrystallized dolomites and limestones on top. Akdeniz and Ercan (1988) defined the petrography and geochemistry of metarhyolites in the Hasköy Formation and suggested that these metarhyolites are Early Jurassic in age based on the fossil content of the associated sedimentary layers. Erdoğan and Güngör (1992), in a different interpretation, considered this Mesozoic succession as the uppermost part of the Menderes Massif and suggested a new stratigraphy consisting of the Late Triassic–Campanian Kayaaltı Formation in the lower part and the Late Cretaceous (?Maastrichtian) Hasköy Formation on top. Erdoğan and Güngör (1992) described metarhyolites in the Hasköy Formation composed of red and green metaclastics. Konak and Çakmakoğlu (2007) named this sequence the Akhisar Nappe and redefined its internal stratigraphy based on the fossil content (*Thecosmilia* cf. *clatharata*) as follows: (1) the Triassic metaclastic rocks with metarhyolites and metaconglomerates in the lower part (Hasköy Formation) and (2) Early Jurassic to Cretaceous recrystallized carbonates with rudists at the top (Görenez Limestone).

The internal stratigraphy and tectonic setting of the Akhisar Nappe resemble those of the Mesozoic part of the Afyon Zone. However, no correlation between these units has been established and the western continuation of the Afyon Zone remains unclear. The present study documents the internal stratigraphy and tectonic setting of the Akhisar Nappe and correlates it to the Afyon Zone based on new data on stratigraphy, fossil records, geochemistry, geochronology, and kinematics.

## 2. Materials and methods

The carbonate sequence cropping out to the east of Akhisar was mapped and paleontologically sampled along two stratigraphic sections. The methodology of kinematic analysis includes systematic descriptions and measurements of the mesoscopic shear criteria in outcrops oriented perpendicular to the foliation and parallel to the associated stretching lineation, and examinations of microscopic structures in oriented thin sections. Seven representative and fresh samples from the metarhyolites were geochemically analyzed and their major geochemical affinities and tectonic settings were discussed. Major oxide and trace element compositions were determined by inductively coupled plasma-atomic emission spectrometer (ICP-AES) following $LiBO_2$ fusion and dilute nitric acid digestion. Loss on ignition is by weight difference after ignition at 1000 °C. Rare earth element (REE) analyses were conducted by inductively coupled plasma-mass spectrometer (ICP-MS) in the ACME Analytical Laboratories in Vancouver, Canada.

We studied the petrography and geochemistry of the metarhyolites in the Akhisar Nappe, and dated them by U–Pb (zircon, laser ablation) method. In U–Pb zircon geochronology in metarhyolites, 28 zircon grains from one sample were separated and analyzed. A rock sample weighing 10–15 kg was processed in the Sample Preparation Laboratory of the Department of Geological Engineering, Dokuz Eylül University, using standard mineral separation techniques. Each rock sample was crushed to coarse sand size with a tungsten carbide jaw crusher. Afterwards, zircons were concentrated by flotation using a shaking table, sieving, magnetic separation, and heavy liquids. A representative batch of 28 zircon crystals with grain sizes of 150–300 µm was manually picked and mounted in Araldite 2020 resin.

U–Pb isotopic data were obtained at Goethe University Frankfurt by laser ablation sector field inductively coupled plasma mass spectrometry (LA-SF-ICP-MS) employing a Thermo-Finnigan Element2 mass spectrometer coupled to a Resolution S-155 (Resonetics) 193 nm ArF Excimer laser (CompexPro 102, Coherent) equipped with a two-volume ablation cell (Laurin Technic, Australia). The laser was operated at 5.5 Hz at a 176 fluence of about <2 J $cm^{-2}$. This yielded with the above configuration at a spot size of 30 µm and depth penetration of 0.6 µm $s^{-1}$ a sensitivity of 14,000 cps/g $g^{-1}$ for $^{238}U$. All age data presented here were obtained by single spot analyses with a spot diameter of 30 µm and a crater depth of approximately 15–20 µm. The methods employed for analysis and data processing are described in detail by Gerdes and Zeh (2006) and Frei and Gerdes (2009). For quality control, the Plešovice (Sláma et al., 2008) and 91500 (Wiedenbeck et al., 1995) zircon reference materials were analyzed, and our results were consistently in excellent agreement with the published ID-TIMS ages. The calculation of concordia ages and plotting of concordia diagrams were performed using Isoplot/Ex 3.0 (Ludwig, 2003). All uncertainties are reported at the 2s level.

## 3. Results

The present study describes the internal stratigraphy of the Akhisar Nappe by analyzing fossil contents from recrystallized carbonates, absolute U–Pb zircon ages of the metarhyolites, and the kinematic features along its lower contact around Akhisar (Figure 2). These new data enable a clearer correlation between the Akhisar Nappe and the Afyon Zone. The Mesozoic succession explored in the study closely resembles previously reported sequences in the Afyon Zone (Figure 2) in western and central Anatolia. Thus, the stratigraphy and tectonic position, fossil content within the carbonate sections, and the geochemical and radiogenic characteristics of the metarhyolites in the Akhisar Nappe align with the typical sequences of the Afyon Zone. This correlation sheds light on the presence of the Afyon Zone while clarifying the blurred geological map of the Akhisar region.

### 3.1. Internal stratigraphy of the Akhisar Nappe

The Akhisar Nappe, named by Konak and Çakmakoğlu (2007), is represented by a very low-grade metasedimentary sequence in which the lower part is named the Hasköy Formation and the upper part is named the Görenez Limestone. The Hasköy Formation consists of yellow, pale brown, green, and red metapelites and metapsammites (Figure 2). In this detrital part, metaconglomerate intercalations, recrystallized gray limestones, and metarhyolite intercalations are present.

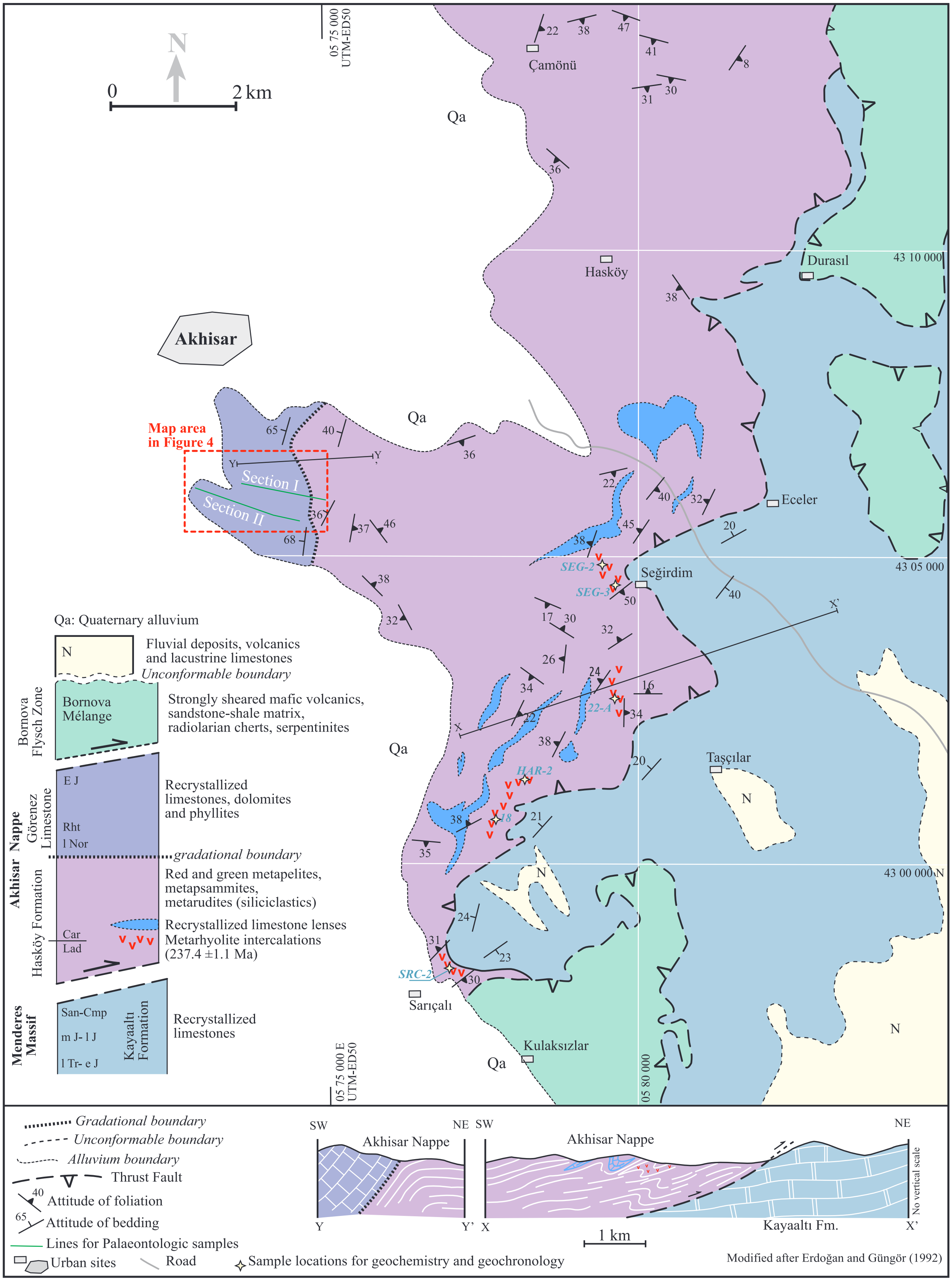


**Figure 2.** Geologic map and cross-sections of the Akhisar region.

Metaconglomerate lenses in the metapsammites and metapelites are composed of quartz conglomerates with pebbles embedded in a sericite-muscovite-rich sandy matrix, which shows an elongation parallel to the foliation planes. The age and stratigraphic position of the Hasköy Formation were inferred as Early Jurassic by Akdeniz et al. (1980) and Latest Cretaceous by Erdoğan and Güngör (1992). The Görenez Limestone is located on top of the Hasköy Formation with a gradational contact and is represented by a carbonate section composed of recrystallized limestones and dolomites (Figures 3 and 4a–4c). The overlying recrystallized carbonate sequence was mapped as Jurassic to Late Cretaceous Görenez Limestone by Akdeniz et al. (1980), while it was reinterpreted as the lateral equivalent of the Kayaaltı Formation as a part of the Menderes Massif by Erdoğan and Güngör (1992).

The metaclastic sequence with metarhyolite intercalations and recrystallized limestone lenses of the Hasköy Formation passes gradually upward into a sheared and recrystallized carbonate sequence of the Görenez Limestone. In the present study, we measured and sampled the Görenez Limestone along two sections to the southeast of Akhisar (Figures 2 and 4a). The fossil contents of the upper carbonate section reveals the stratigraphic positions of underlying metaclastics and overlying recrystallized carbonates. Along section I, the sequence starts at the base with red metapelites with metaconglomerate lenses of the Hasköy Formation, and grades upward into yellow-pinkish white, clayey dolomitic limestones with white-gray clayey dolomitic limestone and gray recrystallized limestone interlayers (Figure 4a). Along the uppermost levels, the sequence ends with strongly deformed, sheared recrystallized limestones. Along this section, dolomitic limestones and recrystallized limestones show grainstone, packstone, and wackestone textures and contain crinoids, foraminifera, and algae (Figures 5a–5c). The upper part of this carbonate succession measured along section I was followed along a different section (section II) approximately 500 m south of section I (Figure 4c). The carbonate succession measured along section II starts at the base with lateral continuation of strongly sheared gray limestones of section I (Figure 4b) and passes gradually upward into white dolomites, dark gray-black recrystallized dolomites, gray recrystallized dolomites, massive dolomites, and micritic limestones (Figure 4c). The dolomites (5 in Figure 5a) and limestones in this section are grainstone (2 and 9 in Figure 5a) and wackestone in texture (1, 3, 4, 6, 7, 8, 10, and 11 in Figure 5a). From the points of lithology, facies, and stratigraphic position, the recrystallized carbonates of the Görenez Limestone closely resemble the recrystallized limestones of the Budağan Limestones found at the top of the İkibaşlı Formation (Akay et al., 2011) in the Kütahya-Emet region.

In section I, along the gradual contact between the metaclastic unit and clayey dolomitic limestones and further upward a fossil association of *Aulotortus friedli*, *Gandinella*? sp., *Aulotortus* sp., *Aulotortus communis*, *Aulotortus* cf. *impressus*, *Aulotortus tumidus*, *Aulotortus* gr. *sinuosus*, *Triasina hantkeni*, Dasyclad algae, and *Gandinella*? sp. is determined (Figure 5b), yielding a late Norian–Rhaetian age for the lower part of the Görenez Limestone. Upward, from dark gray-black dolomites to micritic limestones along section II, a fossil association of Textularid foraminifera, *Siphovalvulina gibralterensis*, *Duotaxis* cf. *metula*, *Lituosepta cf. recoarensis*, *Paleomayncina termieri*, *Everticyclammina praevirguliana*, *Endotriadella* sp., *Reophax* sp., *Mesoendothyra* sp., *Riyadhella* sp., *Meandrovolota asiagoensis*, and *Paleodasycladus mediterraneous* is determined (Figure 5c), suggesting an Early Jurassic age for the upper part of the Görenez Limestone (Figure 3).

### 3.2. Geochemistry and geochronology of the metarhyolites

The metarhyolites are found as intercalations within the Hasköy Formation represented by a metaclastic sequence in the Akhisar Nappe (Figure 3). White, pale green, yellow rhyolitic lavas present a porphyritic texture showing euhedral to subhedral quartz phenocrystals in a strongly sheared glassy matrix. The major and trace element compositions of these rhyolites are provided in Table 1. In the diagram of $Zr/TiO_2$*0.0001 versus $SiO_2$ by Winchester and Floyd (1977) leucocratic lava intercalations in metaclastics indicate rhyolite–rhyodacite composition (Figure 6a) and a postcollisional rift-related intraplate nature (Figures 6b and 6c). The normalized trace element characteristics of the metarhyolites are given in Figure 6d and Figure 6e. In the primitive mantle-normalized trace elements patterns (Figure 6d) and primitive mantle-normalized REE patterns (Figure 6e), a distinct enrichment with a negative trend in light REEs (LREE) and a slight enrichment and almost flat trends in heavy REEs (HREE) are clear (Figure 6e). This negative trend from LREEs to HREEs shows concordance with the REE pattern seen in crustal magmas.

We employed LA-ICP-MS U–Pb dating analysis of 28 zircon grains from the metarhyolites in the present study to determine the age of volcanism (Table 2). The external morphology and internal textures of zircon crystals are predominantly euhedral, transparent, and colorless to pale pink (Figures 7a and 7b). Most of them are short prismatic and long prismatic tetragonal crystals. They show variable sizes ranging from 50 to 200 µm. Most of them contain fluid inclusions. The most abundant group of the zircon crystals belong to (101) pyramids and (110) prisms, which show zircon subtypes of G1 and L5 (Figure 7a, population 1). According to Pupin (1980, 1988), they crystallized

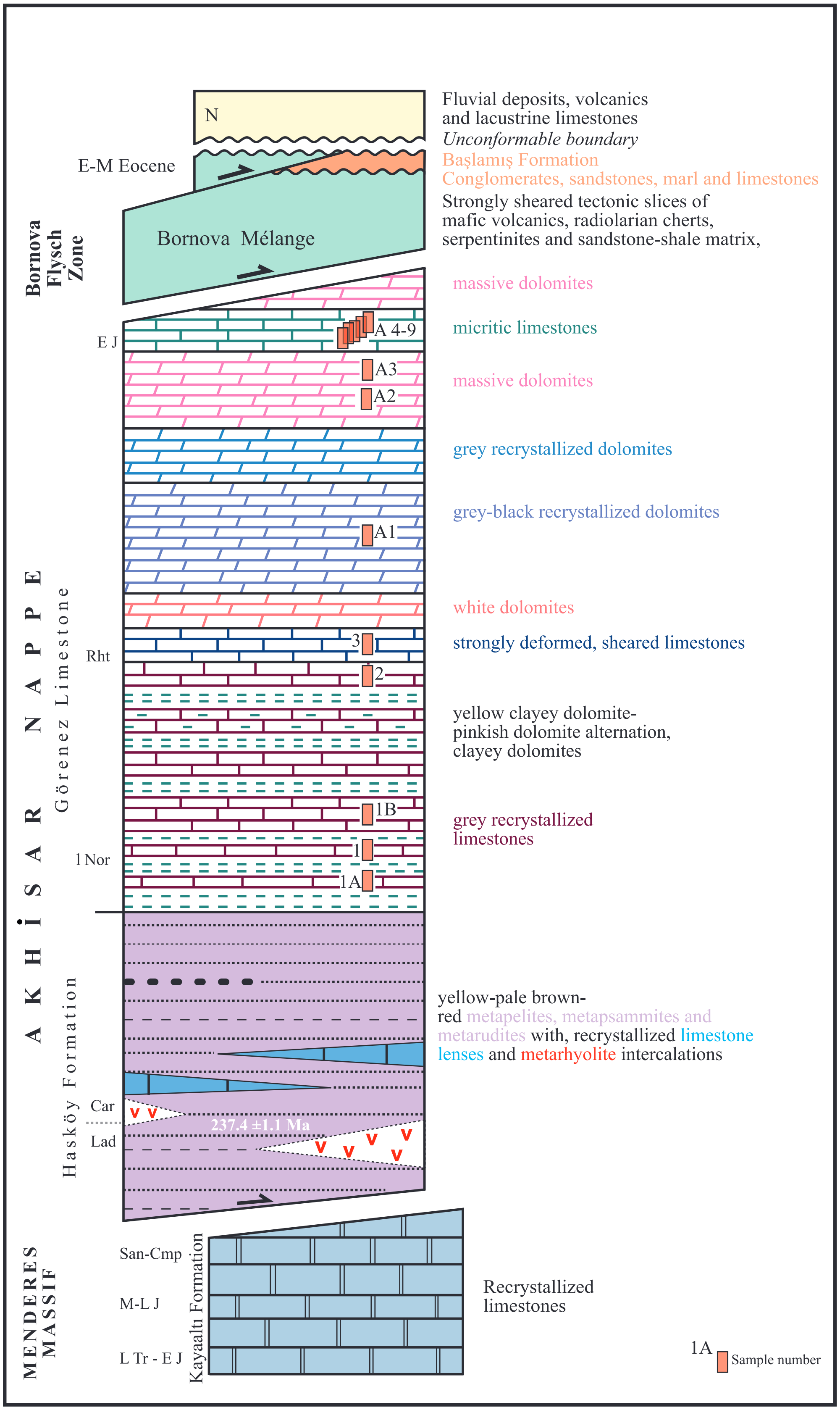


**Figure 3.** Stratigraphic section of the Akhisar Nappe.

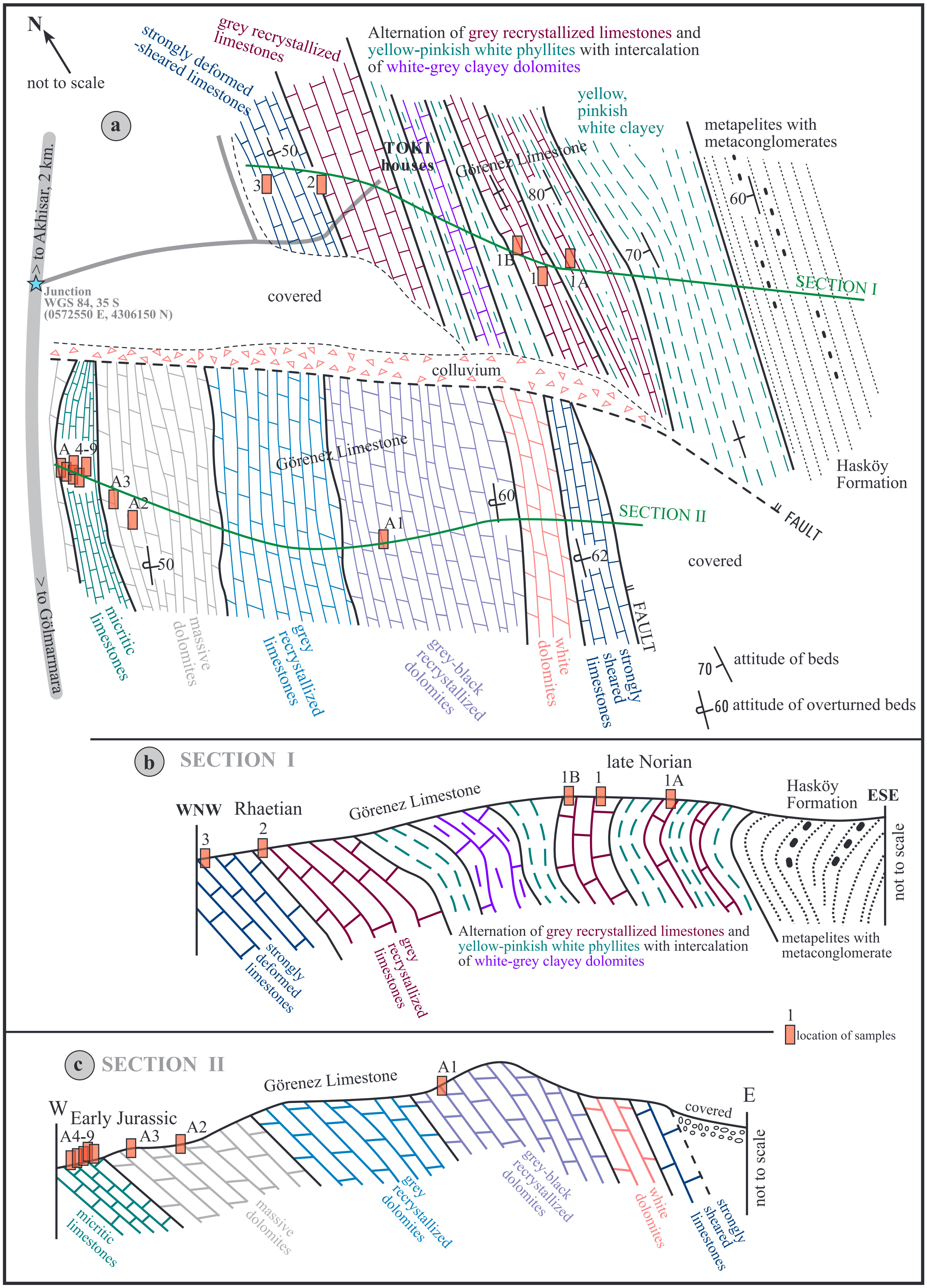


**Figure 4.** a) Simplified geological map and b–c) cross sections showing stratigraphic positions of samples with fossils.

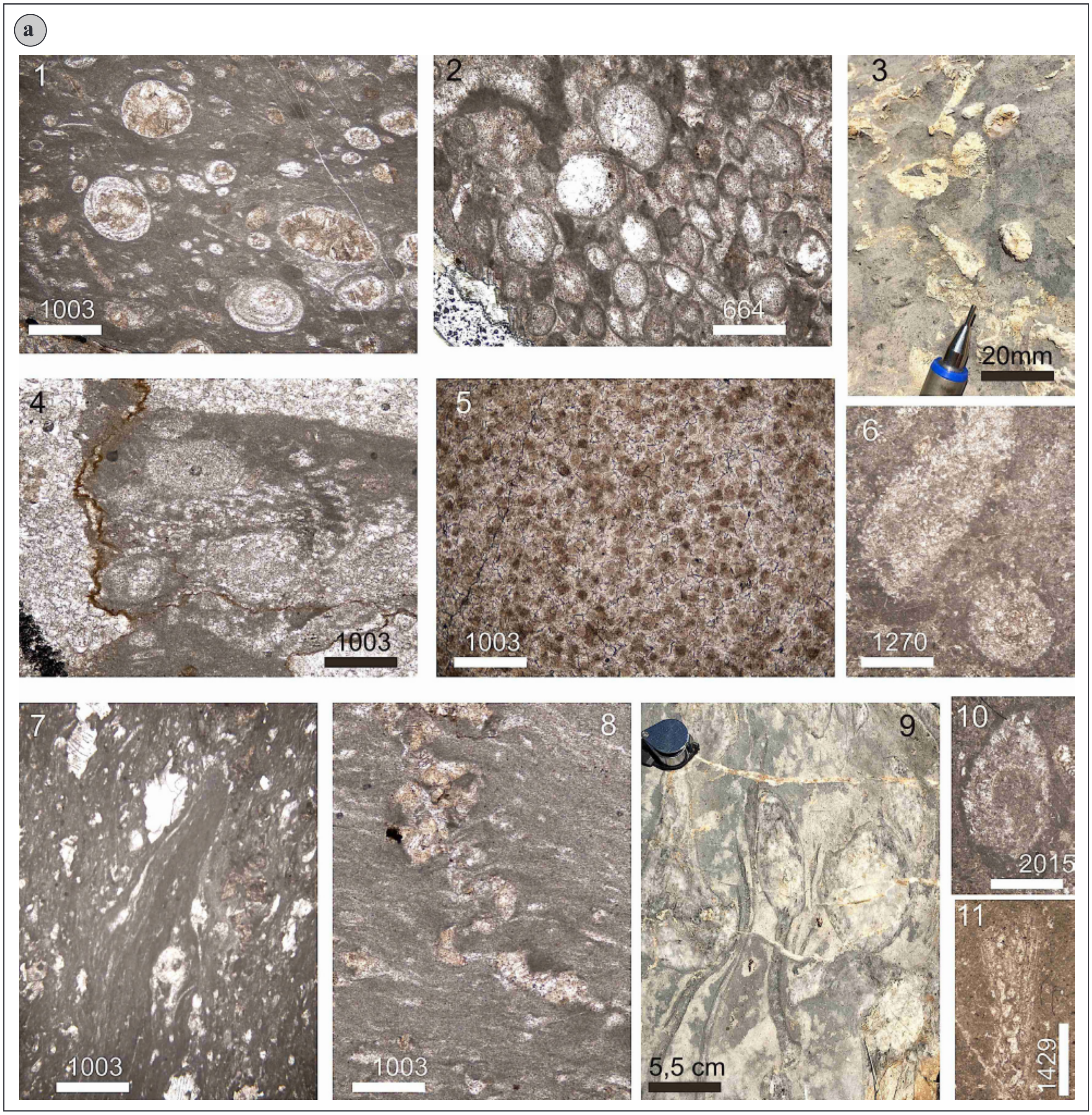


**Figure 5.** a) Microscopic views of Norian–Rhaetian (1–5 and 9) and Early Jurassic (6–8, 10, and 11) carbonates. 1: foraminifer-bearing wakestone, 2: foraminifer-bearing packstone, 3: coral-bearing recrystallized limestone, 4: dolomitic limestone, 5: dolostone consisting of dolospar crystals, 6, 10, and 11 extremely recrystallized probable *Paleodasycladus mediterraneus* individuals, 7 and 8: extremely stretched and recrystallized limestones, 9: probably crinoid-bearing recrystallized limestone (scale bars except 3 and 9 are in micrometers).

at around 600 °C. Population 2 represents the second type of zircon crystals in metarhyolites, which belong to (101)<<(211) pyramids and (100)>>(110) prisms. They have zircon subtypes of L1, which crystallized at about 600 °C. Population 3 (Figure 7a inset) corresponds to relict core-bearing xenocrystic zircon crystals, which seem to be inherited from an older mantle source. These morphological subtypes of the zircon population, according to Pupin's morphological scale (Pupin, 1988), are typical of zircon from aluminous monzogranitic and granodioritic magmas.

The concordia age diagram based on $^{206}Pb/^{238}U$ versus $^{207}Pb/^{235}U$ plots for metarhyolite samples is given in Figure 7c. Due to the inherited zircon cores within population 3

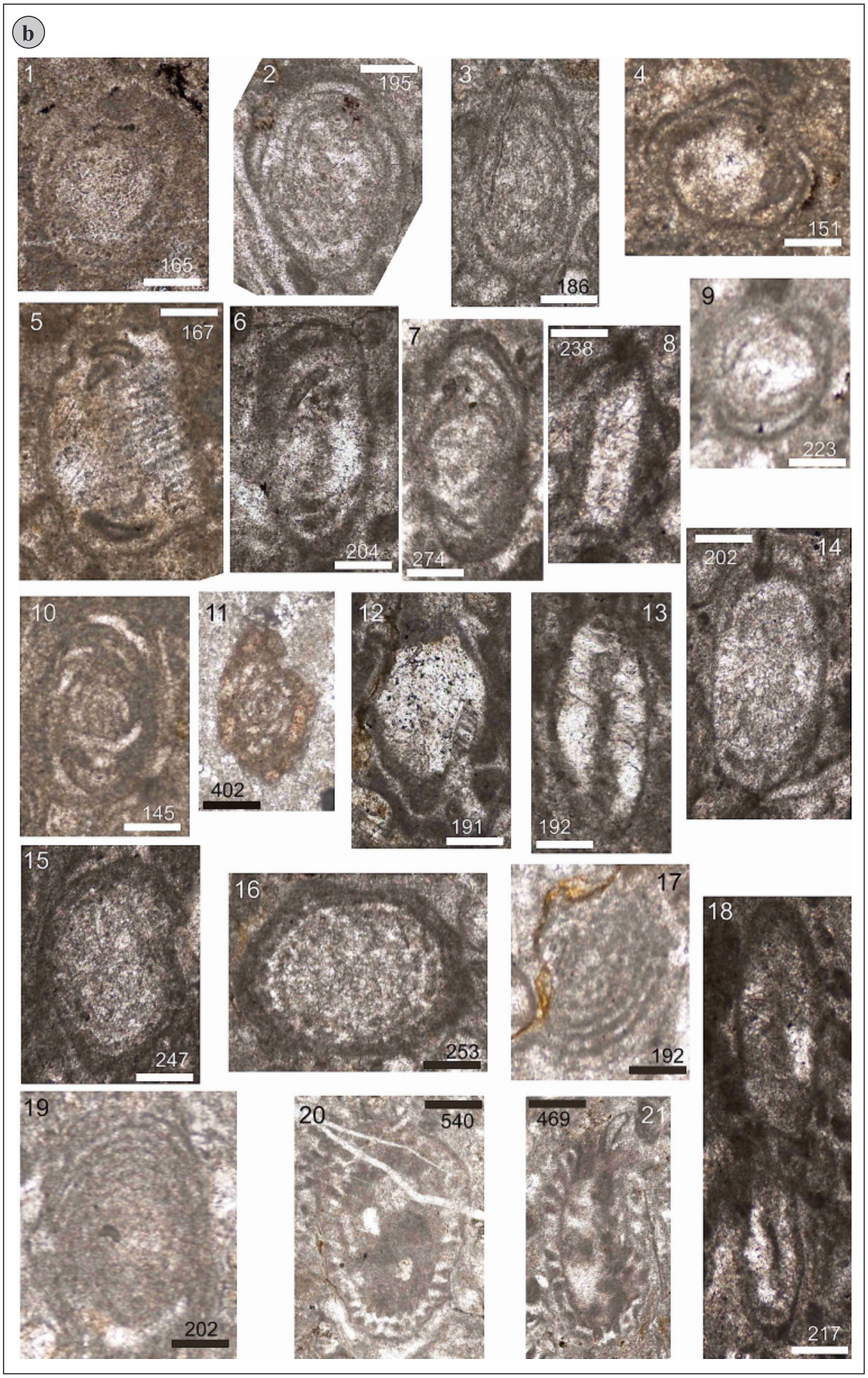


**Figure 5.** b) Microscopic views of Norian–Rhaetian foraminifera and algae. 1–4 and 9: *Aulotortus friedli*, 5–7 and 14: *Aulotortus* gr. *sinuosus*, 8 and 18: *Aulotortus tumidus*, 10 and 11: *Gandinella* sp., 12: *Aulotortus communis*, 13: *Aulotortus* cf. *impressus*, 15–17 and 19: *Triasina hantkeni*, 20 and 21 Dasyclad algae (scale bars: micrometers).

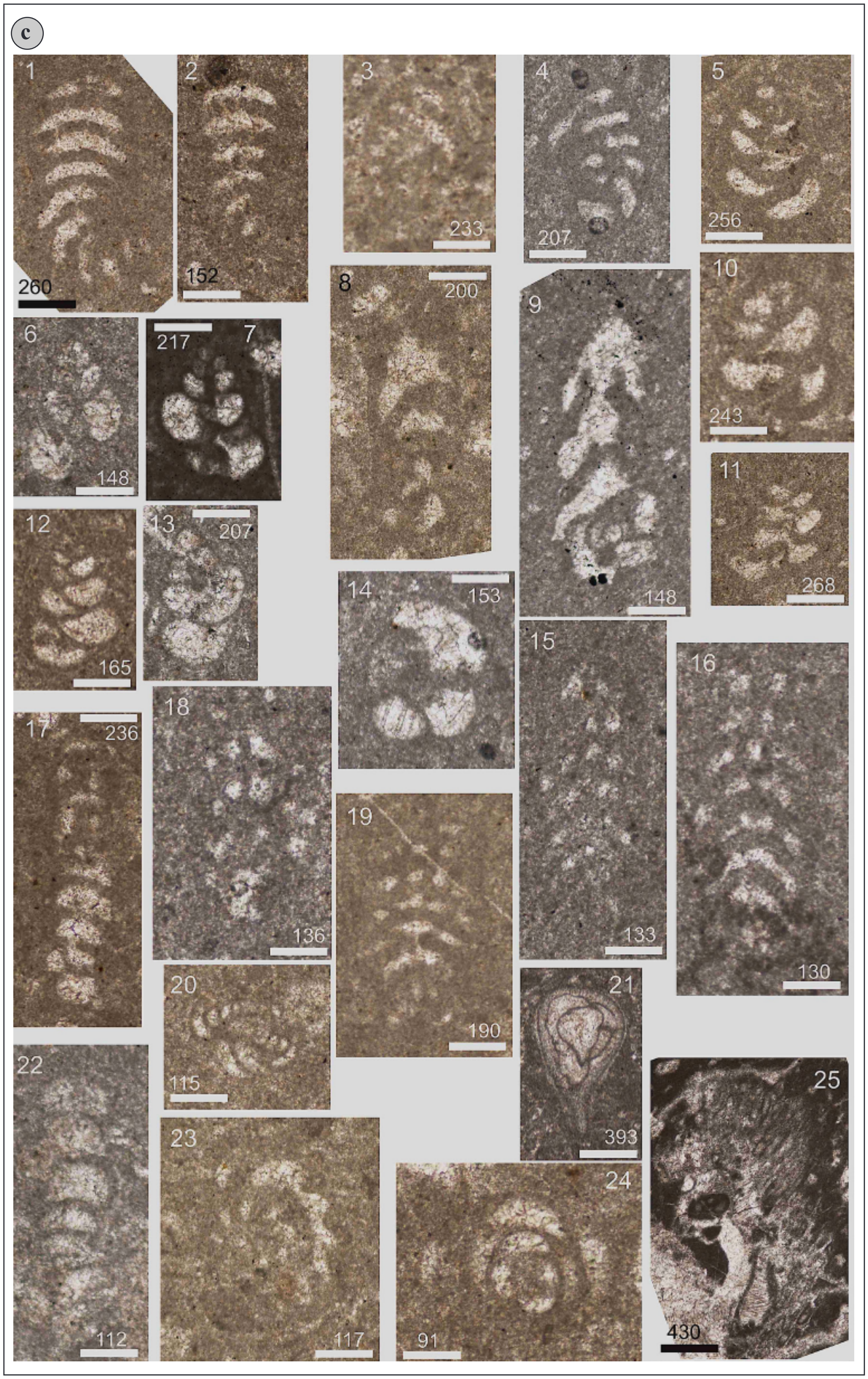


**Figure 5.** c) Microscopic views of the Early Jurassic foraminifers and algae. 1–4: *Paleomayncina termieri*, 5, 10, and 11: *Riyadhella* sp., 6, 7, 12, and 13: *Siphovalvulina gibralterensis*, 8: *Reophax* sp., 9: *Everticyclammina praevirguliana*, 14: *Duotaxis* cf. *metula*, 15, 16, 18, and 19: *Lituosepta* cf. *recoarensis*, 17 and 22: *Endotriadella* sp., 20 and 24: *Meandrovolota asiagoensis*, 21: *Thaumatoporella parvovesiculifera*, 23: *Mesoendothyra* sp., 25: *Paleodasycladus mediterraneous* (scale bars: micrometers).

**Table 1**. Major oxides (% wt) and trace element contents (ppm) of the metarhyolites in the Hasköy Formation.

| Samples | 18 | 22A | HAR2 | HAR3 | SEG2 | SEG3 | SRC2 |
|---|---|---|---|---|---|---|---|
| **SiO2** | 73.01 | 72.14 | 74.17 | 72.01 | 74.32 | 75.87 | 72.38 |
| **Al2O3** | 14.33 | 11.61 | 14.15 | 14.48 | 13.30 | 14.49 | 12.74 |
| **Fe2O3** | 1.14 | 0.52 | 0.29 | 2.16 | 0.69 | 0.56 | 1.70 |
| **MgO** | 0.39 | 0.27 | 0.26 | 0.65 | 0.29 | 0.27 | 0.44 |
| **CaO** | 0.04 | 3.48 | 0.87 | 0.41 | 1.08 | 0.29 | 1.87 |
| **Na2O** | 0.33 | 1.39 | 5.32 | 1.98 | 2.26 | 1.44 | 1.89 |
| **K2O** | 9.14 | 6.73 | 3.24 | 5.81 | 5.31 | 4.61 | 5.91 |
| **TiO2** | 0.10 | 0.06 | 0.05 | 0.09 | 0.07 | 0.06 | 0.14 |
| **P2O5** | 0.02 | 0.03 | 0.02 | 0.02 | 0.03 | 0.02 | 0.04 |
| **MnO** | <0.01 | 0.04 | 0.01 | 0.02 | 0.01 | <0.01 | 0.03 |
| **Cr2O3** | 0.005 | 0.006 | 0.003 | 0.006 | 0.004 | 0.003 | 0.007 |
| **LOI** | 1.3 | 3.5 | 1.5 | 2.2 | 2.5 | 2.3 | 2.7 |
| **Sum** | 99.86 | 99.86 | 99.88 | 99.88 | 99.90 | 99.93 | 99.88 |
| **Mo** | 0.2 | 0.3 | 0.4 | 0.1 | 0.2 | <0.1 | 0.1 |
| **Cu** | 1.4 | 10.2 | 51.6 | 0.9 | 4.1 | 0.6 | 1.6 |
| **Pb** | 1.8 | 9.7 | 46.1 | 1.8 | 7.6 | 3.7 | 6.9 |
| **Zn** | 4 | 27 | 2 | <1 | <1 | <1 | 1 |
| **Ni** | 3.1 | 7.7 | 5.0 | 3.4 | 3.3 | 1.8 | 5.1 |
| **Tl** | <0.1 | 0.1 | <0.1 | <0.1 | <0.1 | <0.1 | 0.1 |
| **Co** | 40.1 | 37.5 | 30.1 | 25.4 | 20.2 | 16.3 | 20.9 |
| **Cs** | 4.9 | 2.9 | 1.6 | 6.7 | 5.7 | 5.7 | 4.6 |
| **Ga** | 20.9 | 15.2 | 19.0 | 21.1 | 14.0 | 18.7 | 16.1 |
| **Hf** | 3.1 | 2.6 | 3.2 | 3.6 | 3.0 | 2.6 | 3.1 |
| **Nb** | 17.5 | 15.4 | 19.5 | 17.9 | 10.2 | 12.7 | 14.0 |
| **Rb** | 163.2 | 82.8 | 66.3 | 151.8 | 117.4 | 122.0 | 157.5 |
| **Sn** | 2 | 2 | 3 | 2 | 1 | 1 | 2 |
| **Sr** | 47.8 | 174.1 | 59.4 | 66.9 | 27.9 | 8.2 | 110.6 |
| **Ta** | 1.1 | 1.4 | 1.9 | 1.4 | 0.7 | 0.9 | 1.1 |
| **Th** | 20.9 | 12.5 | 10.0 | 21.7 | 15.3 | 8.3 | 18.3 |
| **U** | 4.6 | 7.4 | 8.4 | 3.5 | 3.5 | 3.1 | 4.5 |
| **V** | <8 | <8 | <8 | 15 | <8 | <8 | 19 |
| **W** | 344.9 | 273.2 | 197.2 | 185.8 | 173.1 | 73.6 | 182.4 |
| **Zr** | 91.3 | 61.9 | 59.8 | 87.7 | 79.8 | 61.4 | 88.0 |
| **Y** | 12.3 | 9.6 | 6.9 | 8.2 | 6.4 | 4.9 | 12.6 |
| **La** | 13.6 | 6.4 | 3.2 | 8.1 | 13.8 | 4.8 | 19.6 |
| **Ce** | 30.4 | 13.8 | 5.6 | 17.6 | 27.0 | 9.5 | 39.4 |
| **Pr** | 3.53 | 1.72 | 0.60 | 2.06 | 3.12 | 1.13 | 4.58 |
| **Nd** | 12.8 | 6.7 | 2.2 | 7.2 | 11.1 | 4.0 | 17.1 |
| **Sm** | 2.95 | 1.92 | 0.73 | 1.71 | 2.14 | 0.84 | 3.40 |
| **Eu** | 0.70 | 0.51 | 0.21 | 0.41 | 0.56 | 0.26 | 0.79 |
| **Gd** | 2.54 | 1.86 | 0.89 | 1.39 | 1.54 | 0.87 | 2.76 |
| **Dy** | 2.11 | 1.65 | 1.16 | 1.39 | 1.02 | 0.80 | 1.94 |
| **Tb** | 0.38 | 0.30 | 0.18 | 0.24 | 0.21 | 0.14 | 0.37 |
| **Ho** | 0.39 | 0.32 | 0.24 | 0.29 | 0.20 | 0.16 | 0.38 |
| **Er** | 1.07 | 0.87 | 0.67 | 0.87 | 0.56 | 0.44 | 1.04 |
| **Tm** | 0.18 | 0.14 | 0.12 | 0.12 | 0.09 | 0.08 | 0.16 |
| **Yb** | 1.11 | 0.87 | 0.83 | 0.90 | 0.56 | 0.52 | 1.10 |
| **Lu** | 0.16 | 0.12 | 0.11 | 0.14 | 0.09 | 0.08 | 0.15 |

**Table 1**. (Continued.)

| | | | | | | | |
|---|---|---|---|---|---|---|---|
| **Mg#** | 40.42 | 50.73 | 64.00 | 37.37 | 45.46 | 48.88 | 33.91 |
| **(La/Yb)N** | 8.79 | 5.28 | 2.77 | 6.46 | 17.68 | 6.62 | 12.78 |
| **(La/Sm)N** | 2.98 | 2.15 | 2.83 | 3.06 | 4.16 | 3.69 | 3.72 |
| **(Gd/Yb)N** | 1.89 | 1.77 | 0.89 | 1.28 | 2.27 | 1.38 | 2.08 |
| **Eu*** | 15.44 | 10.66 | 4.55 | 8.69 | 10.24 | 4.82 | 17.28 |
| **Eu/Eu*** | 0.78 | 0.83 | 0.80 | 0.81 | 0.94 | 0.93 | 0.79 |

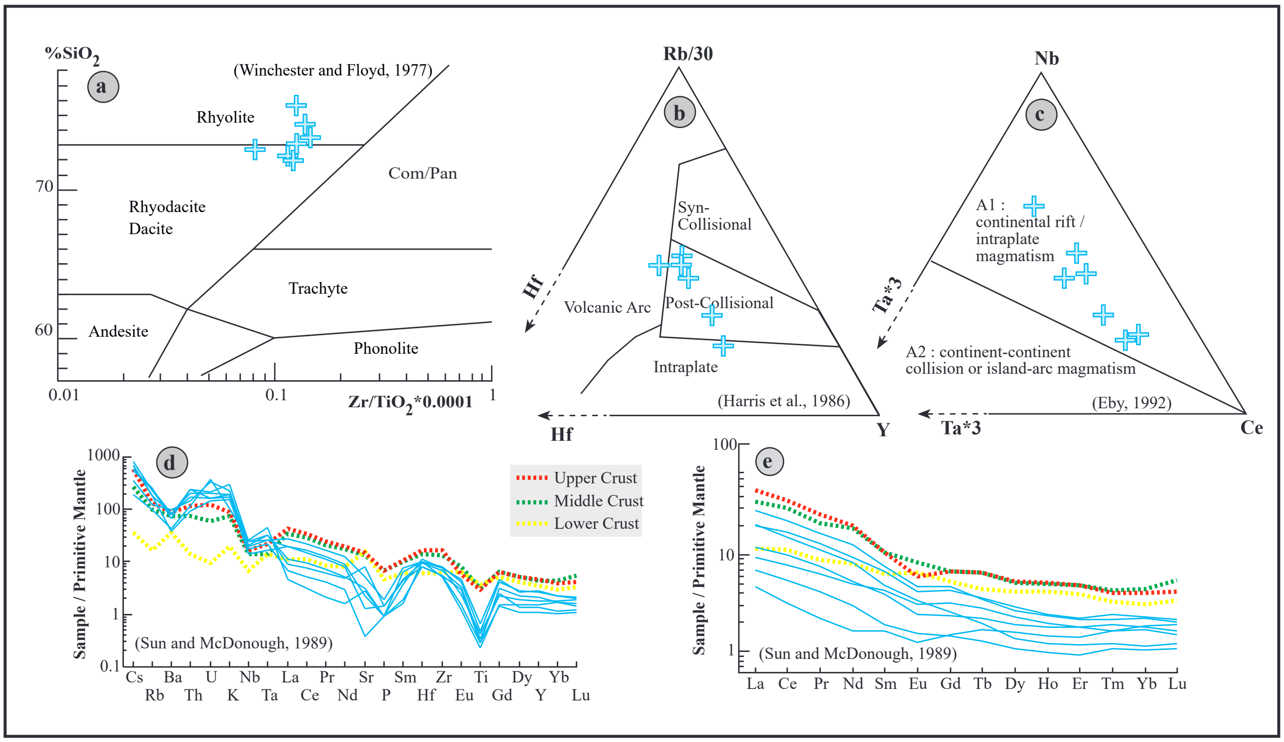


**Figure 6.** a) Nomenclature, b and c) tectonic setting, d and e) spider diagrams of the metarhyolites in the Hasköy Formation.

(Figure 7a), the U–Pb ages of them are scattered and their age ellipsoids were in concordance along the concordia (1018 ± 16 Ma, 688 ± 14 Ma, 803 ± 12 Ma, and 372 ± 34 Ma), indicating that the source of rhyolitic magma is a Proterozoic and Late Devonian crust. A cluster of 19 grains from populations 1 and 2 (Figures 7a and 7b) defines a significant concordant U–Pb zircon age of 237.4 ± 1.1 Ma (Ladinian–Carnian transition) with MSWD = 1.3 (Figure 7c), which is interpreted as a crystallization age. These new radiogenic age data indicate that rhyolite intercalations in the lower part of the Hasköy Formation are early Late Triassic in age, but not Early Jurassic as interpreted by Akdeniz et al. (1980) and Akdeniz and Ercan (1988). In addition, the fossil contents of the recrystallized limestones along the upper contact of the Hasköy Formation indicate an age of Late Triassic (late Norian–Rhaetian). Only the uppermost part of the carbonate section of Akhisar Nappe contains fossils indicating an Early Jurassic age (Figures 5a–5c). Therefore, the age of the Hasköy Formation is confirmed to be early Late Triassic by radiogenic data, and the age of the carbonates on top of the Hasköy Formation is determined to be late Norian–Early Jurassic based on the fossil record.

### 3.3. Kinematics of the Akhisar Nappe

The field-based kinematic dataset from the Akhisar Nappe is based on descriptions and systematic measurements of mesoscopic shear criteria in outcrops oriented perpendicular to foliation and parallel to associated lineation, and analysis of microstructures in oriented thin sections. The present paper documents structural data measured at 63 observation points along the fault zone between the Hasköy and Kayaaltı formations. In the Akhisar Nappe, a very low grade metamorphism is identified by rough foliation and absence of cataclastic

**Table 2**. U–Th–Pb isotope data of the metarhyolites in the Hasköy Formation.

| grain | 207Pb[a] (cps) | U[b] (ppm) | Pb[b] (ppm) | $\frac{Th^b}{U}$ | 206Pb[c] (%) | $\frac{^{206}Pb^d}{^{238}U}$ | ±2σ (%) | $\frac{^{207}Pb^d}{^{235}U}$ | ±2σ (%) | $\frac{^{207}Pb^d}{^{206}Pb}$ | ±2σ (%) | rho[e] | $\frac{^{206}Pb}{^{238}U}$ | ±2σ (Ma) | $\frac{^{207}Pb}{^{235}U}$ | ±2σ (Ma) | $\frac{^{207}Pb}{^{206}Pb}$ | ±2σ (Ma) | conc.[f] (%) |
|---|---|---|---|---|---|---|---|---|---|---|---|---|---|---|---|---|---|---|---|
| A506 (core) | 14141 | 370 | 30.8 | 1.09 | 0.7 | 0.05908 | 9.4 | 0.4671 | 11.2 | 0.05734 | 6 | 0.85 | 370 | 34 | 389 | 37 | 505 | 131 | 73 |
| A507 | 10958 | 943 | 36.1 | 0.91 | 0.4 | 0.03386 | 1.9 | 0.2375 | 2.3 | 0.05087 | 1.3 | 0.82 | 215 | 4 | 216 | 5 | 235 | 31 | 91 |
| A508 | 30099 | 1352 | 58.6 | 0.66 | 4.6 | 0.03742 | 2 | 0.2607 | 2.6 | 0.05053 | 1.6 | 0.77 | 237 | 5 | 235 | 5 | 220 | 38 | 108 |
| A509 | 13321 | 1086 | 44.2 | 0.81 | 0.6 | 0.03764 | 1.9 | 0.2636 | 2.4 | 0.0508 | 1.4 | 0.81 | 238 | 4 | 238 | 5 | 232 | 32 | 103 |
| A512 | 15394 | 1078 | 44.4 | 0.7 | 1.4 | 0.0382 | 1.9 | 0.2666 | 2.5 | 0.05061 | 1.6 | 0.76 | 242 | 5 | 240 | 5 | 223 | 37 | 108 |
| A514 | 12129 | 1022 | 41.5 | 0.69 | 1.5 | 0.03791 | 2 | 0.2672 | 2.6 | 0.05111 | 1.7 | 0.75 | 240 | 5 | 240 | 6 | 246 | 40 | 98 |
| A515 | 26165 | 1759 | 68.8 | 0.69 | 2 | 0.03763 | 2.1 | 0.2636 | 2.7 | 0.05081 | 1.8 | 0.75 | 238 | 5 | 238 | 6 | 232 | 42 | 103 |
| A516 | 26572 | 2239 | 85.8 | 0.43 | 0.4 | 0.03801 | 2 | 0.2655 | 2.4 | 0.05067 | 1.4 | 0.81 | 240 | 5 | 239 | 5 | 226 | 32 | 107 |
| A517 | 19553 | 1262 | 50.7 | 0.76 | 3.2 | 0.03712 | 2 | 0.259 | 2.4 | 0.0506 | 1.3 | 0.84 | 235 | 5 | 234 | 5 | 223 | 31 | 105 |
| A518 | 9868 | 770 | 29.8 | 0.49 | 0.3 | 0.03753 | 2 | 0.2646 | 2.3 | 0.05113 | 1.2 | 0.85 | 237 | 5 | 238 | 5 | 247 | 28 | 96 |
| A519 | 7990 | 627 | 23.6 | 0.71 | 0.7 | 0.03469 | 1.9 | 0.2428 | 2.3 | 0.05075 | 1.3 | 0.83 | 220 | 4 | 221 | 5 | 230 | 30 | 96 |
| A520 (core) | 30688 | 662 | 76.5 | 0.5 | 1 | 0.1128 | 2.1 | 0.9779 | 3.2 | 0.06288 | 2.5 | 0.65 | 689 | 14 | 693 | 16 | 704 | 53 | 98 |
| A521 | 44211 | 606 | 33.1 | 0.56 | 1.6 | 0.03955 | 4.3 | 0.3673 | 6.5 | 0.06736 | 4.9 | 0.66 | 250 | 11 | 318 | 18 | 849 | 102 | 29 |
| A522 | 18285 | 1457 | 54.7 | 0.56 | 0.4 | 0.03651 | 1.9 | 0.2545 | 2.5 | 0.05055 | 1.6 | 0.77 | 231 | 4 | 230 | 5 | 220 | 36 | 105 |
| A523 | 7951 | 601 | 23.3 | 0.42 | 0.3 | 0.03803 | 1.9 | 0.2679 | 2.7 | 0.05109 | 1.9 | 0.71 | 241 | 5 | 241 | 6 | 245 | 44 | 98 |
| A524 (core) | 9180 | 118 | 22.1 | 0.79 | 0 | 0.171 | 2 | 1.726 | 2.5 | 0.07321 | 1.5 | 0.79 | 1018 | 18 | 1018 | 16 | 1020 | 31 | 100 |
| A525 | 12584 | 274 | 17 | 2.01 | 7.1 | 0.03689 | 3.3 | 0.2599 | 3.9 | 0.05109 | 2 | 0.86 | 234 | 8 | 235 | 8 | 245 | 46 | 95 |
| A526 | 29612 | 1451 | 60.2 | 0.57 | 4.5 | 0.03711 | 2 | 0.2587 | 2.5 | 0.05056 | 1.6 | 0.77 | 235 | 5 | 234 | 5 | 221 | 37 | 106 |
| A527 | 9221 | 761 | 30.3 | 0.6 | 0.2 | 0.03765 | 2 | 0.2655 | 2.6 | 0.05115 | 1.6 | 0.78 | 238 | 5 | 239 | 6 | 247 | 37 | 96 |
| A529 (core) | 31961 | 465 | 58.4 | 0.09 | 0.2 | 0.1328 | 2 | 1.205 | 2.2 | 0.06579 | 0.98 | 0.89 | 804 | 15 | 803 | 12 | 800 | 21 | 101 |
| A530 | 11497 | 700 | 29.5 | 1.17 | 1.5 | 0.0379 | 2.5 | 0.2698 | 3 | 0.05164 | 1.6 | 0.84 | 240 | 6 | 243 | 6 | 269 | 37 | 89 |
| A531 | 85905 | 1815 | 91.8 | 1.64 | 11.9 | 0.03383 | 1.9 | 0.2381 | 3.8 | 0.05103 | 3.3 | 0.51 | 215 | 4 | 217 | 8 | 242 | 76 | 89 |
| A533 | 11648 | 426 | 18.6 | 1.47 | 7.2 | 0.03383 | 2.2 | 0.2391 | 3.2 | 0.05126 | 2.2 | 0.7 | 214 | 5 | 218 | 6 | 252 | 52 | 85 |
| A534 | 27014 | 457 | 26.3 | 0.75 | 2.4 | 0.03755 | 3.8 | 0.2615 | 4.1 | 0.05052 | 1.6 | 0.92 | 238 | 9 | 236 | 9 | 219 | 38 | 109 |
| A535 | 75630 | 4282 | 168.9 | 0.32 | 1.7 | 0.03798 | 2 | 0.2671 | 2.5 | 0.051 | 1.5 | 0.79 | 240 | 5 | 240 | 5 | 241 | 35 | 100 |
| A536 | 13513 | 1091 | 41.4 | 0.46 | 0.6 | 0.037 | 1.9 | 0.2596 | 2.8 | 0.05089 | 2.1 | 0.68 | 234 | 4 | 234 | 6 | 236 | 47 | 99 |
| A539 | 28477 | 1120 | 52.1 | 1.02 | 6.7 | 0.03712 | 2 | 0.2618 | 2.9 | 0.05115 | 2 | 0.7 | 235 | 5 | 236 | 6 | 248 | 47 | 95 |

**Table 2**. (Continued.)

| | | | | | | | | | | | | | | | | | | | |
|---|---|---|---|---|---|---|---|---|---|---|---|---|---|---|---|---|---|---|---|
| A541 | 20680 | 1073 | 45.6 | 0.6 | 2.9 | 0.03785 | 2.3 | 0.2615 | 2.9 | 0.0501 | 1.7 | 0.79 | 239 | 5 | 236 | 6 | 200 | 40 | 120 |
| OG **g** | 210608 | 35 | 34.8 | 1.09 | 1.66 | 0.71134 | 2 | 29.25 | 2.6 | 0.29826 | 1.9 | 0.92 | 3463 | 55 | 3462 | 26 | 3461 | 29 | 100 |
| Ples. **g** | 33921 | 1502 | 80 | 0.15 | 2 | 0.05367 | 1.8 | 0.3939 | 2.4 | 0.05323 | 1 | 0.75 | 337 | 6 | 337 | 7 | 339 | 24 | 100 |
| Felix **g** | 18792 | 322 | 38 | 2.12 | 0.45 | 0.08095 | 2.5 | 0.6404 | 3.4 | 0.05738 | 2.1 | 0.6 | 502 | 12 | 503 | 13 | 506 | 46 | 99 |

Spot size = 30 µm, depth of crater 15–20 µm. $^{206}Pb/^{238}U$ error is the quadratic additions of the within run precision (2 SE) and the external reproducibility (2 SD) of the reference zircon. $^{207}Pb/^{206}Pb$ error propagation ($^{207}Pb$ signal dependent) following Gerdes and Zeh (2009). $^{207}Pb/^{235}U$ error is the quadratic addition of the $^{207}Pb/^{206}Pb$ and $^{206}Pb/^{238}U$ uncertainty.

**a**: Within run background-corrected mean $^{207}Pb$ signal in cps (counts per second).

**b**: U and Pb content and Th/U ratio were calculated relative to GJ-1 reference zircon.

**c**: percentage of the common Pb on the $^{206}Pb$. b.d. = below detection limit.

**d**: corrected for background, within-run Pb/U fractionation (in case of $^{206}Pb/^{238}U$) and common Pb using Stacy and Kramers (1975) model Pb composition and subsequently normalized to GJ-1 (ID-TIMS value/measured value); $^{207}Pb/^{235}U$ calculated using $^{207}Pb/^{206}Pb/(^{238}U/^{206}Pb*1/137.88)$

**e**: rho is the $^{206}Pb/^{238}U/^{207}Pb/^{235}U$ error correlation coefficient.

**f**: degree of concordance = $^{206}Pb/^{238}U$ age / $^{207}Pb/^{206}Pb$ age × 100

**g**: Accuracy and reproducibility were checked by repeated analyses (n = 25) of reference zircon OG, Plešovice, and Felix; data given as mean with 2 standard deviation uncertainties

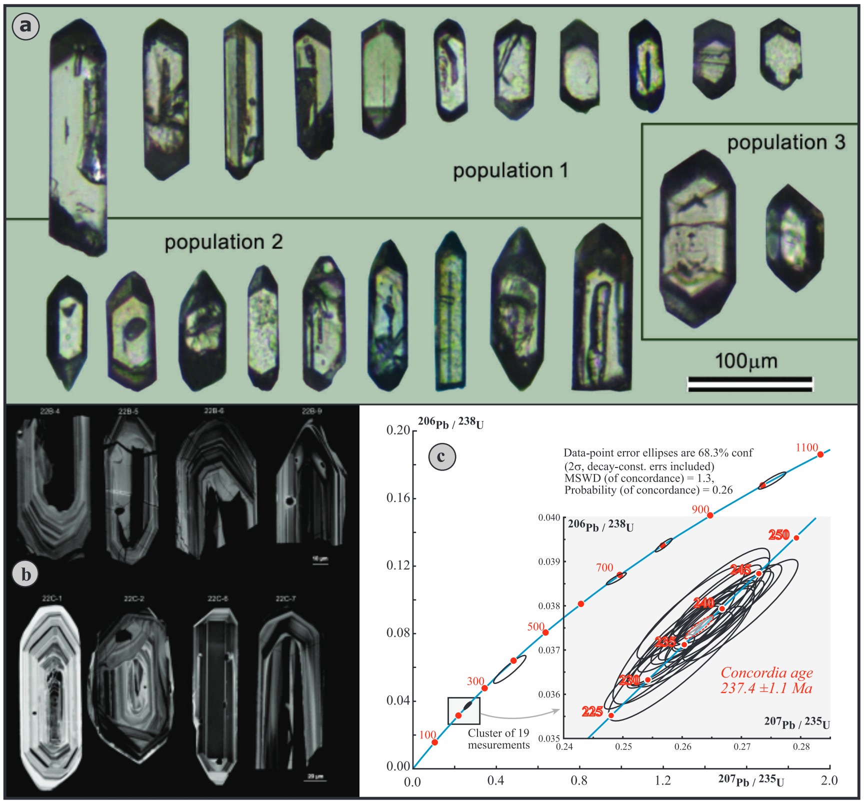


**Figure 7.** a) Binocular microphotograph showing zircon populations in the metarhyolites, b) Concordia diagram displaying the U–Pb data obtained by LA-ICP-MS for magmatic zircons, c) CL images of representative zircons of the metarhyolites in the Hasköy Formation.

texture at microscale in the metaclastic lower part of the Hasköy Formation. The intensity of deformation increases toward the contact zone between the Akhisar Nappe and the Kayaaltı Formation. Therefore, this contact zone and the damage zones in both the hanging wall and footwall rocks provide data for kinematic analysis. The sericite and chlorite crystals in cleavage domains and mica beards around the coarse grains define the rough foliation. The foliation plane is identified by the preferred orientation of tiny micas in the metapelites and flattened quartz and feldspar grains in the metapsammites. The flattened limestone pebbles in the metaconglomerates mark the foliation planes. Along the lower contact of the Hasköy Formation, the metarhyolites show mylonitic foliation, which is identified by elongated and flattened phenocrystals of feldspar and quartz. In the recrystallized limestone lenses, the preferred orientation of the fine grained calcite crystals shows prominent continuous foliation.

The long axis of the deformed pebbles, elongated quartz and feldspar, and orientation of calcite crystals identify linear fabric along the lower contact of the Hasköy Formation. The recrystallized limestone lenses within the Hasköy Formation are fine grained and gray and show continuous foliation with prominent stretching lineation marked by a linear array of fibrous, white calcite crystals along the foliation planes (Figure 8a). The intraformational limestone conglomerates contain strained and elongated pebbles (Figure 8b). In the metarhyolites, stretching lineation is identified by strongly elongated quartz and feldspar phenocrystals (Figure 8c). The channel-fill conglomerates contain quartzite, rhyolite, and sandstone pebbles and sand matrix. The white rhyolite and quartzite pebbles show prominent elongation and stretching (Figure 8d). The systematic measurements of the linear fabric in red metapelites, metapsammites, metarudites, recrystallized limestones, and metarhyolites in the lower part of the Hasköy Formation are concentrated at 028/14 and 231/12 (Figure 9). The main trend of linear fabric indicates that the Akhisar Nappe was emplaced along the SW–NE direction on the Kayaaltı Formation. Some minor NW-trending linear fabric could be related to the postemplacement local rotations due to overprinting faults or folding during the progressive emplacement of the Akhisar Nappe. The calcite fibers (Figure 10a) and linear array of dolomite clasts (Figure 10b) along the foliation planes of recrystallized limestones signify a linear fabric along the upper contact of the Kayaaltı Formation. The asymmetric boudinage of dolomite layers (Figures 10c and

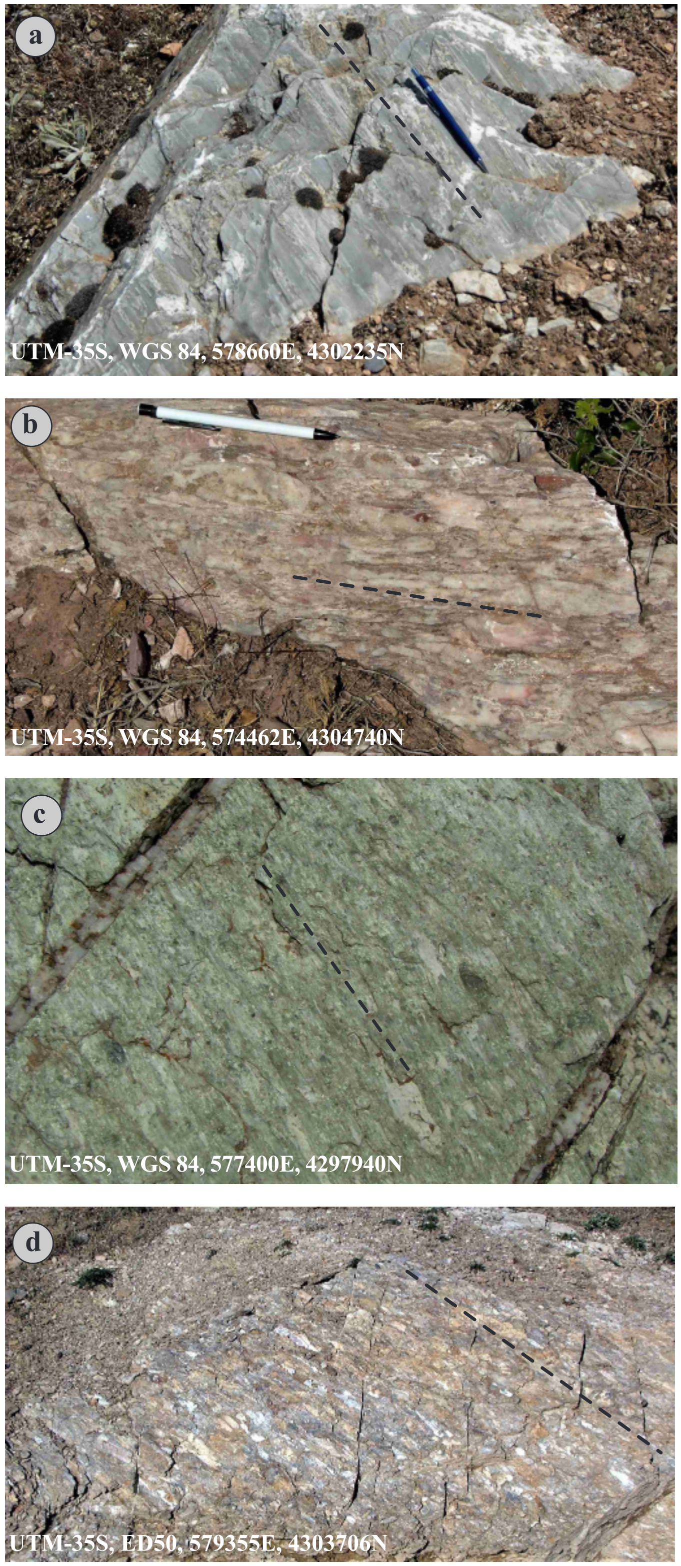


**Figure 8.** Photographs showing foliation and linear fabric in the Akhisar Nappe. Field view of foliation and linear fabrics along base of the Hasköy Formation. a) Strongly sheared recrystallized limestones with foliation and lineation, b) limestone metaconglomerates with strongly elongated pebbles, c) metarhyolite with mylonitic foliation and lineation, d) metaconglomerates with stretched pebbles. Pencils in a and b are 15 cm. Width of views in c and d are 25 cm and 2 m, respectively. Black dashed lines are parallel to the stretching lineation.

10d) in the fault zone in the Kayaaltı Formation clearly indicate top-to-the-northeast sense of shear. In addition to these structures, the fault zone along the lower part of the Akhisar Nappe contains sigma clasts (Figure 11a), asymmetrically deformed quartz pebbles (Figure 11b) in channel-fill conglomerates, S/C structures (Figure 11c) in oriented thin sections from metarhyolites, and overturned mesoscopic folds (Figure 11d) in the metapelite and metapsammite alternation. These asymmetric structures define a top-to-the-northeast sense of shear during emplacement of the Akhisar Nappe.

In the Akhisar region, the latest movement of the Bornova Mélange is inferred by internal structures and boundary relations of the Early–Middle Eocene Başlamış Formation extending in a narrow zone between Akkocalı and Başlamış villages located 30 km northeast of Akhisar. The Başlamış Formation unconformably covers the strongly sheared rocks of the Bornova Mélange along laterally discontinuous basal conglomerates composed mainly of ophiolite fragments (Akdeniz, 1980) derived from the Bornova Mélange. Local overthrust of the Bornova Mélange onto the Başlamış Formation and upright subhorizontal, closed folds in the Early–Middle Eocene sequence suggest syn- and postdepositional nappe emplacements in the Akhisar region.

### 3.4. Correlation of the Akhisar Nappe

In western and central Anatolia, on top of the Menderes Massif and Taurides, the Mesozoic lithostratigraphy of the Afyon Zone (Figure 12) is consistently represented by detritics in the lower parts (Hasköy Formation, İkibaşlı Formation, and Karaova Formation) and platform carbonates (Görenez Limestone, Budağan Limestone, Gereme Formation, and Ula Marbles) in the upper parts (Figure 12). Our study introduces a tectonic slice of the Afyon Zone along the northwest border of the Menderes Massif in the Akhisar region (Figure 12a). The Akhisar Nappe clearly shows a lithostratigraphy similar to those in the Afyon Zone in the Kütahya, Afyon, Konya, and Bodrum regions around the northern, eastern, and southern flanks of the Menderes Massif, respectively. The lower part of the Akhisar Nappe is composed of Triassic red metaclastics with metarhyolite intercalations (237.4 ± 1.1 Ma) and limestone lenses, and its upper section consists of Late Triassic–Early Jurassic recrystallized limestones (Figure 12a). To the north of the Menderes Massif between Balıkesir and Kütahya (Figure 12b), the

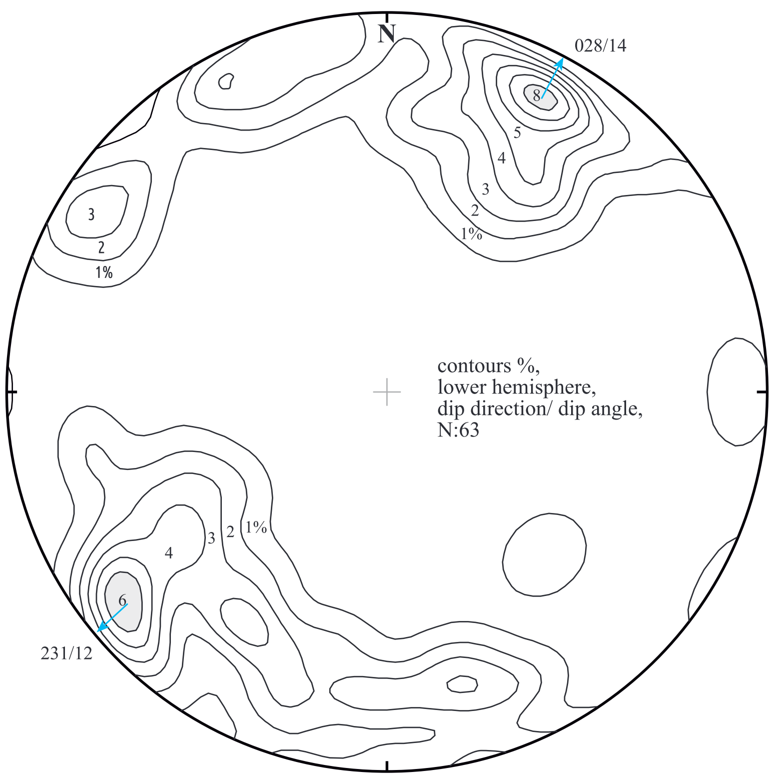


**Figure 9.** Contour diagram of the linear fabric measured along the contact zone between the Hasköy Formation (Afyon Zone) and the Kayaaltı Formation (Menderes Massif). In the Akhisar Nappe, the measurements of linear fabrics are from the metapelites, metarhyolites, metaconglomerates, and recrystallized limestones within the Hasköy Formation.

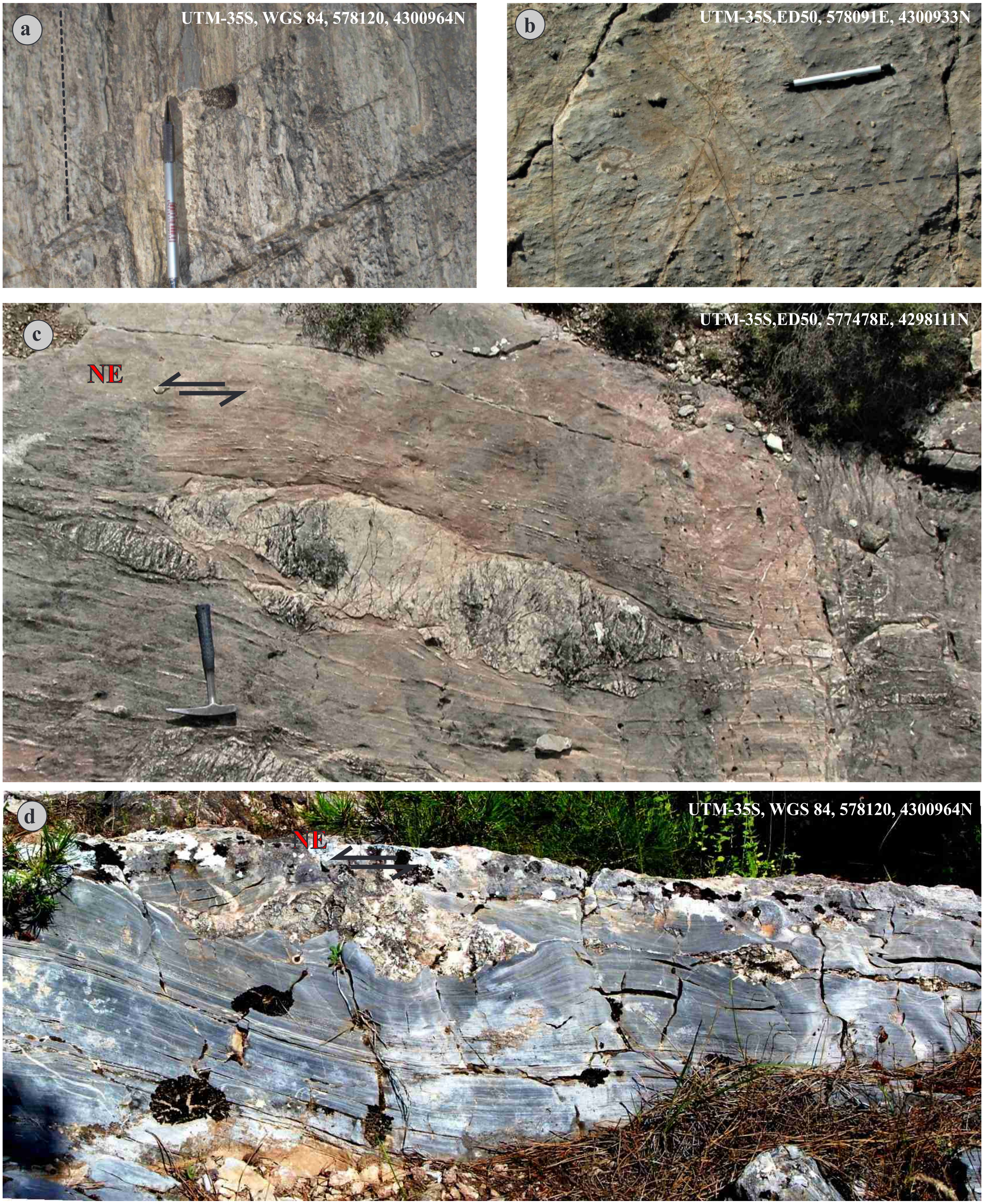


**Figure 10.** Photographs showing the linear fabric and shear sense indicators along the upper contact of the Kayaaltı Formation composed of metacarbonates. a) The linear fabric marked by stretched calcite crystals. b) The lineation designated by trains of dolomite clasts along the boudinage of white dolomite layers in pink recrystallized limestones. d) Asymmetric boudinage of white dolomite layer in very fine grained, gray recrystallized limestones. Pencils are 15 cm in a and b, hammer is 33 cm in c, width of view is 5 m in d.

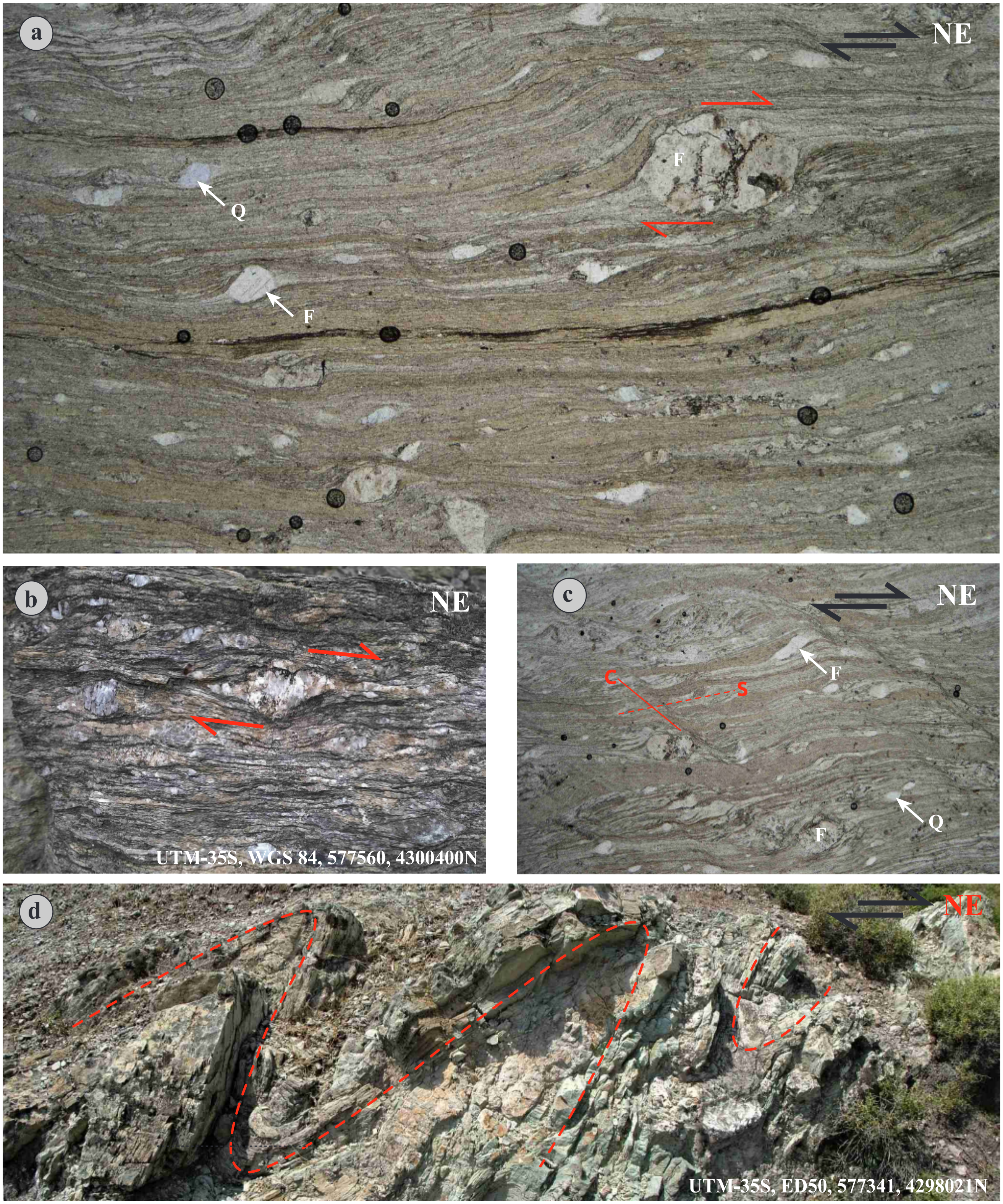


**Figure 11.** a) Photomicrograph showing sigma clast with a top-to-the-NE sense of shear in metarhyolites. b) Photograph showing asymmetrically deformed pebble in the metaconglomerate in the Hasköy Formation. The asymmetry of tails clearly shows a top-to-the-NE sense of shear. c) Photomicrograph showing S/C relation in the metarhyolites. d) Photograph showing overturned folds (red dashed line) with NE-vergence in the red and green metapelites in the Hasköy Formation along the lower contact of the Akhisar Nappe. F: Feldspar, Q: Quartz. Width of views 2 mm in a and c, 15 cm in b, 10 m in d.

Afyon Zone is represented by the Middle–Late Triassic İkibaşlı Formation composed of phyllites and schists with laterally discontinuous metaconglomerates, recrystallized limestone, and metarhyolite intercalations in the lower part and Early Jurassic–Kimmeridgian platform limestones (Budağan Limestone) in the upper part (Kaya, 1972; Akdeniz and Konak, 1979a, 1979b; Kaya et al., 1995; Candan et al., 2005; Akay et al., 2011). In central Anatolia, in the Sızma (Konya) region (Figure 12c), metatrachyandesites unconformably cover an Early Carboniferous sequence made up of metasiliciclastics with limestone and black chert lenses, and blocks of volcanic rocks (Akal et al., 2012). Pourteau et al. (2010, 2013, 2016) mapped the southwestward continuation of the Afyon Zone on top of the Menderes Massif and Cycladic Blueschists (Figures 1 and 12d). In this region, in ascending order, the carpholite-bearing (Rimmelé, 2003, Rimmelé et al., 2003a) Permo-Triassic, red and green metaclastic rocks without volcanic intercalation (Karaova Formation), Middle–Late Jurassic dolomites (Gereme Formation), and rudist-bearing (Özer et al., 2017) Cretaceous limestones and cherty limestones (Ula Marbles) form the Ören Tectonic Slice of the Afyon Zone. The Mesozoic section of the Afyon Zone represents a passive margin of the Anatolide–Tauride Belt (Okay, 1984,

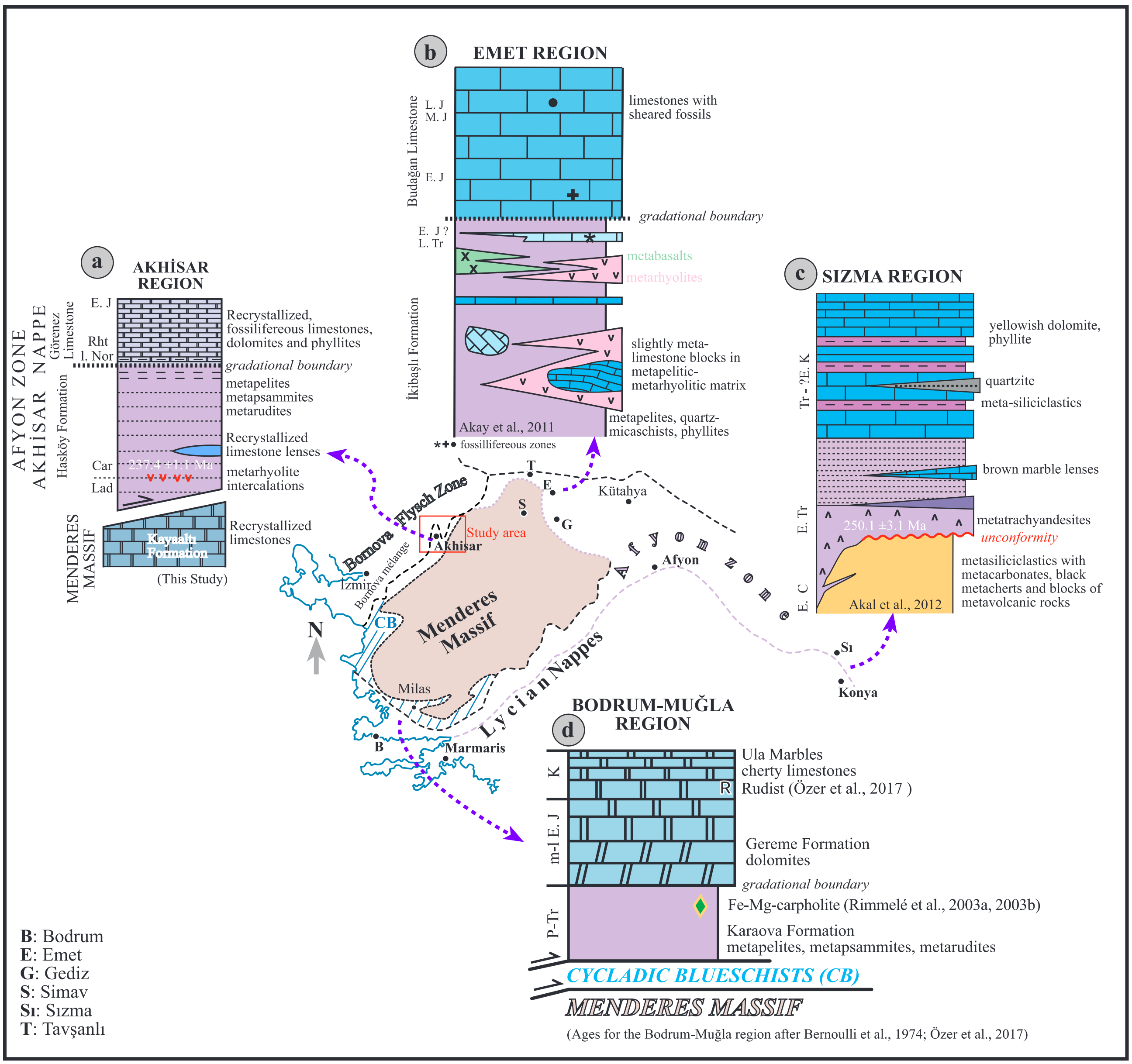


**Figure 12.** Simplified stratigraphic sections of some tectonic slices in the Afyon Zone that surround the Menderes Massif and Cycladic Blueschists.

1986; Candan et al., 2005) and is composed of a siliciclastic sequence with volcanic intercalations in the lower part and recrystallized limestones in the upper part.

The lithostratigraphy and tectonic position of the Akhisar Nappe resemble all those parts of the Afyon Zone along the Anatolide–Tauride belt. In contrast to these lithostratigraphic similarities, the Akhisar Nappe shows a very low grade metamorphism diagnosed by tiny micas (sericites) along cleavage domains of rough foliation in the metasiliciclastics of the Hasköy Formation. The tectonic slices of the Afyon Zone along the north, east, and south flanks of the Menderes Massif show HP/LT metamorphism (~350 °C and 6–9 kbar, ~30 km depth) (Rimmelé et al., 2003a, 2003b; Okay, 2004; Candan et al., 2005; Pourtaeu et al., 2010, 2013). Moreover, along the south and east flanks of the Menderes Massif, the siliciclastic lower part of the Ören Tectonic Slice, as a typical Afyon Zone sequence, is lacking in rhyolite intercalations.

In western Anatolia, the tectonic belts located in close proximity to the Akhisar Nappe contain Triassic leucocratic, acidic intrusives in the Karaburun Belt (Ercan et al., 2000; Erkül et al., 2008; Akal et al., 2010) and in the Menderes Massif around Derbent and Alaşehir (Dannat, 1997; Dannat and Reischmann, 1998; Koralay et al., 2001, 2004, 2011). In the Karaburun Belt, the acidic intrusives show an island arc tectonic setting, while in the Menderes Massif, they show a within plate tectonic setting. The geochemical characteristics of the rhyolites in the Hasköy Formation suggest a mantle-sourced magma strongly affected by continental crust that extruded in a rift setting along the northern edge of the Anatolide–Tauride Block, related to subduction of the Paleo-Tethys.

As with the mapping of the Afyon Zone in the NE-trending zone between İzmir and Balikesir, previous studies display some inadequacies in the mapping of the Cycladic Blueschists. The Cyladic Blueschists are supposed to be along the northwest edge of the Menderes Massif (Pourteau et al., 2010; Çetinkaplan et al., 2020) without a detailed geological map that shows the separating of the Cycladic Blueschists from the Menderes Massif and a detailed description of its metamorphic grade.

**4. Conclusions**

- In the Akhisar region, the Akhisar Nappe is composed of a very low grade metamorphic succession composed of Triassic metaclastic rocks with metarhyolite intercalations and recrystallized limestone lenses in the lower part (the Hasköy Formation), and late Norian–Early Jurassic recrystallized limestones and dolomites (the Görenez Limestones) in the upper part. The age of the Hasköy Formation is revealed as the Late Triassic (237.4 ± 1.1 Ma; Ladinian–Carnian transition), and the age of Görenez Limestones on top of the Hasköy Formation is determined as Late Norian–Early Jurassic by fossil descriptions.
- The new radiogenic data indicate that the metarhyolites in the lower part of the Hasköy Formation are Late Triassic in age, and not Early Jurassic as inferred by Akdeniz et al. (1980) and Akdeniz and Ercan (1988).
- Tectonic slices of the Afyon Zone located along the north, east, and south of flanks of the Menderes Massif and Cycladic Blueschists show HP/LT metamorphism (~350 °C and 6–9 kbar, ~30 km depth, Candan et al., 2005); however, the Akhisar Nappe shows very low grade metamorphism diagnosed by rough foliation with microlithons showing primary detrital textures and cleavage domains marked by tiny sericites.
- Field-based kinematic data measured along the fault zone between the Hasköy Formation (Afyon Zone) and the Kayaaltı Formation (Menderes Massif) indicate that the Akhisar Nappe is emplaced northeastward on the Menderes Massif.
- The internal stratigraphy and tectonic setting of the Akhisar Nappe resemble those of typical Afyon Zone associations along northern, eastern, and southern part of the Menderes Massif and in the Afyon and Konya regions. The description of the Akhisar Nappe in the study area indicates that the Afyon Zone also surrounds the west and northwest edge of the Menderes Massif.

**Acknowledgments**
The Department of Scientific Research Projects of Dokuz Eylül University partly supported this study (project number: 2012.KB.FEN.066). We would like to thank Çağlar Özkaymak for editorial handling and the anonymous reviewers, whose suggestions clarified and strengthened the manuscript

## References


Akal C, Candan O, Koralay OE, Oberhansli R, Chen F (2005) Metavolcanic rocks ın Afyon Zone: implications for Triassic rifting of Neo-Tethyan ocean on Gondwanaland. In: International symposium on the geodynamics of eastern Mediterranean: active tectonics of the Aegean, p 77.

Akal C, Koralay OE, Candan O, Oberhansli R, Chen F (2010). Geodynamic Significance of the Early Triassic Karaburun Granitoid (Western Turkey) for the Opening History of Neo-Tethys: Turkish Journal of Earth Sciences 20: 255-271. https://doi.org/10.3906/yer-1008-1

Akal C, Candan O, Koralay O, Oberhansli R, Chen F et al. (2012). Early Triassic potassic volcanism in the Afyon Zone of the Anatolides/Turkey: Implications for the rifting of the Neo-Tethys. International Journal of Earth Sciences 101: 177-194. https://doi.org/10.1007/s00531-011-0654-2

Akal C, Candan O, Koralay OE, Gerdes A, Oberhansli R (2024). Middle Triassic magmatism in the Afyon Zone of the Anatolides/Eastern Mediterranean: Implications for the extension of the Northern margin of Gondwana and opening of the Inner-Tauride Ocean. Lithos 482-483. https://doi.org/10.1016/j.lithos.2024.107691

Akay E, İşintek İ, Erdoğan B, Hasözbek A (2011). Stratigraphy of the Afyon Zone around Emet (Kütahya, NW Anatolia) and geochemical characteristics of the Triassic volcanism along the northern Menderes Massif. Journal of Mineralogy and Geochemistry 188 (3): 297-316. https://doi.org/10.1127/0077-7757/2011/0205

Akdeniz N, Ercan T (1988). Liassic volcanics in Akhisar (Manisa) region and distribution of Early Mesozoic volcanism around the Aegean Sea. Geological Bulletin of Turkey 31: 33-46.

Akdeniz N, Konak N (1979a). Geology of Simav-Emet-Tavşanlı-Dursunbey-Demirci area. Report of the Mineral Research and Exploration Institute 108 (in Turkish with an abstract in English).

Akdeniz N, Konak N (1979b). Rock units of the Menderes Massif and setting of the metabasic and metaultramafic rocks around Simav. Bulletin of the Geological Society of Turkey 22: 175-184.

Akdeniz N, Konak N, Armağan F (1980). Lower Mesozoic rock units of southeast Akhisar, Manisa. Bulletin of the Geological Congress of Turkey 2: 77-90.

Bernoulli D, De Graciansky PC, Monod O (1974). Extension of the Lycian nappes (SW Turkey) into the southeastern Aegean islands: Eclogae Geolicae Helvatiae 67: 39-90.

Brunn JH, Dumont JF, Graciansky PD, Gutnic M, Juteau T et al. (1971). Outline of the geology of the western Taurides, Campbell, A.S., Ed., Geology and History of Turkey, Tripoli, Libya, Petroleum Exploration Society, 225-255.

Candan O, Çetinkaplan M, Oberhansli R, Rimmelé G, Akal C (2005). Alpine high-p/low-t metamorphism of the Afyon Zone and implications for the metamorphic evolution of western Anatolia, Turkey. Lithos 84: 102-124. https://doi.org/10.1016/j.lithos.2005.02.005

Çetinkaplan M, Candan O, Oberhansli R, Sudo M, Cenki-Tok B (2020). P-T-t evolution of the Cycladic Blueschist Unit in Western Anatolia/Turkey: Geodynamic implications for the Aegean region. Journal of Metamorphic Geology 38 (4): 379-419. https://doi.org/10.1111/jmg.12526

Dannat C (1997). Geochemie, Geochronologie und Nd-Sr-Isotopie der granitoiden Kerngneise des Menderes Massivs SW-Turkei. Dissertation, Johannes Gutenberg-Universitat, Mainz.

Dannat C, Reischmann T (1998). Geochronological, geochemical and isotopic data on granitic gneisses from the Menderes Massif, SW Turkey. 3rd International Turkish Geology Symposium, Ankara, Abstracts, p. 275.

De Graciancky PC (1972). Récherches Géologique dans les Taurus Lycien: PhD thesis, University of Paris-Sud, France (in French).

Eby GN (1992). Chemical subdivision of the A-type granitoids: petrogenetic and tectonic implications. Geology 20 (7): 641-644. https://doi.org/10.1130/0091-7613(1992)020%3C0641:CSOTAT%3E2.3.CO;2

Ercan T, Türkecan A, Satır M (2000). Neogene volcanism of Karaburun Peninsula. In: Proceedings, Cumhuriyetin 75. Yıldönümü Yerbilimleri ve Madencilik Kongresi. Mineral Research and Exploration Institute (MTA) of Turkey, Ankara, 1-18 (in Turkish).

Erdoğan B (1990a). Stratigraphy and tectonic evolution of the İzmir-Ankara Suture Zone between İzmir and Seferihisar. Turkish Association of Petroleum Geologists Bulletin 2 (1): 1-20.

Erdoğan B (1990b). Tectonic relations between İzmir-Ankara Zone and Karaburun Belt. Bulletin of the Mineral Research and Exploration 110: 1-15.

Erdoğan B, Güngör T (1992). Stratigraphy and tectonic evolution of the northern margin of the Menderes Massif. Turkish Association of Petroleum Geologists Bulletin 2: 1-20.

Erkül ST, Sözbilir H, Erkül F, Helvacı C, Ersoy Y et al (2008). Geochemistry of I-type granitoids in the Karaburun Peninsula: West Turkey: Evidence for Triassic continental arc magmatism following closure of the Palaeotethys. Island Arc 17: 394-418. https://doi.org/10.1111/j.1440-1738.2008.00627.x

Frei D, Gerdes A (2009). Precise and accurate in situ U–Pb dating of zircon with high sample throughout by automated LA-SF-ICP-MS. Chemical Geology 261 (3-4): 261-270. https://doi.org/10.1016/j.chemgeo.2008.07.025

Gerdes A, Zeh A (2006). Combined U-Pb and Hf isotope LA-(MC)-ICP-MS analyses of detrital zircons: comparison with SHRIMP and new constraints for the provenance and age of an Armorican metasediment in Central Germany. Earth and Planetary Sciences Letters 249: 47-61. https://doi.org/10.1016/j.epsl.2006.06.039

Gerdes A, Zeh A (2009). Zircon formation versus zircon alteration: new insights from combined U–Pb and Lu-Hf in-situ LA-ICP-MS analyses, and consequences for the interpretation of Archean zircon from the Central Zone of the Limpopo Belt. Chemical Geology 261: 230-243. https://doi.org/10.1016/j.chemgeo.2008.03.005

Göncüoğlu C (1997). Distribution of Lower Paleozoic Units in the Alpine Terranes of Turkey: paleogeographic constraints. In: Göncüoğlu MC and Derman AS (Eds) Lower Palaezoic Evolution in northwest Gondwana, Turkish Association of Petroleum Geologists Special Publication 3: 13-24.

Göncüoğlu MC, Turhan N, Tekin UK (2003). Evidence for the Triassic rifting and opening of the Neotethyan İzmir-Ankara Ocean and discussion on the presence of Cimmerian events at the northern edge of the Tauride-Anatolide Platform, Turkey. Bulletin Geological Society Italy, Special Volume 2: 203-212.

Harris NBW, Pearce JA, Tindle AG (1986). Geochemical characteristics of collision-zone magmatism. In: Coward MP, Ries AC (eds) Collision Tectonics: Geological Society of London, Special Publication 19: 67-81. https://doi.org/10.1144/GSL.SP.1986.019.01.04

Kaya O (1972). Outlines of the ophiolite question in the Tavşanlı Region. Bulletin Geological Society of Turkey 15 (1): 26-108 (in Turkish).

Kaya O, Sadeddin W, Altiner D, Meriç E, Tansel İ et al. (1995). Stratigraphic and structural setting of the anchimetamorphics rocks to the south of Tavşanlı (Kütahya, western Turkey): Relation to the İzmir-Ankara zone. Bulletin of Mineral Research and Exploration 117: 5-16.

Ketin İ (1966). Tectonic units of Anatolia (Asia Minor). Bulletin of the Mineral Research and Exploration 66: 20-34 (in Turkish).

Konak N, Çakmakoğlu A (2007). Discussion on the Menderes Massif and the Mesozoic-Lower Tertiary Sequences in its Close Vicinity in Terms of Tectonic Units. Colloquim on the Menderes Massif in honor of O. Özcan Dora. Extended abstracts Book (ISSN: 978-9944-89-398-5) pp. 56-65.

Koralay OE, Candan O, Akal C, Dora OÖ, Chen F et al. (2011). The Geology and geochronology of Pan-African and Triassic metagranitoids in the Menderes Massif, W-Anatolia, Turkey. Bulletin of Mineral Research and Exploration 142: 69-119.

Koralay OE, Satır M, Dora OÖ (2001). Geochemical and geochronological evidence for Early Triassic calc-alkaline magmatism in the Menderes Massif, western Turkey. International Journal of Earth Sciences 89: 822-835. https://doi.org/10.1007/s005310000134

Koralay OE, Dora OÖ, Chen F, Satır M, Candan O (2004). Geochemistry and geochronology of orthogneisses in the Derbent (Alaşehir) area, Eastern part of the Ödemiş-Kiraz submassif, Menderes Massif: Pan-African magmatic activity. Turkish Journal of Earth Sciences 13 (1): 37-61.

Ludwig K (2003). ISOPLOT 3: a geochronological toolkit for Microsoft excel. Berkeley Geochronology Centre Special Publication 4, 74pp.

Moix P, Beccaletto L, Kozur HW, Hochard C, Rosselet F et al. (2008). A new classification of the Turkish terranes and sutures and its implication for the paleotectonic history of the region: Tectonophysics 451: 7-39. https://doi.org/10.1016/j.tecto.2007.11.044

Okay Aİ (1984). Distribution and characteristics of the northwest Turkey blueschists. In Robertson AHF, Dixon JA (eds.) The geological evolution of the eastern Mediterranean. Journal of Geological Society London, special publication 17: 455-466. https://doi.org/10.1144/GSL.SP.1984.017.01.33

Okay Aİ (1986) High pressure/low temperature metamorphic rocks of Turkey. In: Evans BW, Brown EH (eds.) Blueschists and Eclogites Geological Society of America Memoir No. 164: 333-348.

Okay Aİ (2004). Tectonics and high-pressure metamorphism in northwest Turkey. 32 th International Geological Congress. Field trip guide book. 56 p.

Okay Aİ, Harris NBW, Kelley SP (1998). Exhumation of blueschists along a Tethyan suture in northwest Turkey. Tectonophysics 285: 275-299. https://doi.org/10.1016/S0040-1951(97)00275-8

Okay Aİ, Monod O, Monié P (2002). Triassic blueschists and eclogites from northwest Turkey: vestiges of the Paleo-Tethyan subduction. Lithos 64: 155-178. https://doi.org/10.1016/S0024-4937(02)00200-1

Okay Aİ, Satır M, Maluski H, Siyako M, Monie P et al. (1996). Paleo- and Neo-Tethyan events in northwestern Turkey: Geologic and geochronologic constraints. In: A. Yin and M. Harrison (eds.) The Tectonic Evolution of Asia, Cambridge University Press 420-441.

Okay Aİ, Siyako M, Bürkan KA (1990). Geology and tectonic evolution of the Biga Peninsula (in Turkish). Bulletin of the Turkish Association of Petroleum Geologists 2: 83-121.

Okay Aİ, Tansel İ, Tüysüz O (2001). Obduction, subduction and collision as reflected in the Upper Cretaceous-Lower Tertiary sedimentary record of western Turkey. Geological Magazine 138: 117-142. https://doi.org/10.1017/S0016756801005088

Okay Aİ, Tüysüz O (1999). Tethyan sutures of northern Turkey: Geological Society of London, Special Publication 156: 475-515. http://doi.org/10.1144/GSL.SP.1999.156.01.22

Özcan A, Göncüoğlu MC, Turan N, Uysal Ş, Şentürk K et al. (1988) Late Paleozoic evolution of the Kütahya-Bolkardağ Belt. Middle East Technical University, Journal of Pure and Applied Sciences 21 (1-3) 211-220.

Özer S, Güngör T, Sarı B, Sagular EK, Görmüş M et al. (2017). Cretaceous rudist-bearing platform carbonates from the Lycian nappes (SW Turkey): Rudist associations and depositional setting. Createaceous Research 79: 122-145. https://doi.org/10.1016/j.cretres.2017.07.016

Özgül N (1976). Some geological aspects of the Taurus orogenic belt (Turkey). Bulletin of the Geological Society of Turkey 19: 65-78.

Parlak O, Delaloye M (1999). Precise 40Ar/39Ar ages from the metamorphic sole of the Mersin ophiolite (southern Turkey). Tectonophysics, 301: 145-158. http://doi.org/10.1017/S0016756805001524

Pourteau A, Candan O, Oberhansli R (2010). High-pressure metasediments in central Turkey: constraints on the Neotethyan closure history. Tectonics 29 (5): 18. TC5004. http://doi.org/10.1029/2009TC002650

Pourteau A, Sudo M, Candan O, Lanari P, Vidal O et al. (2013). Neotethys closure history of Anatolia: insights from $^{40}$Ar–$^{39}$Ar geochronology and P–T estimation in high-pressure metasedimentary rocks. Journal of Metamorphic Geology 31 (6): 585-606. https://doi.org/10.1111/jmg.12034

Pourteau A, Oberhansli R, Candan O, Barrier E, Vrielynck B (2016). Neotethyan closure history of western Anatolia: A geodynamic discussion. International Journal of Earth Sciences 105 (1): 203-224. https://doi.org/10.1007/s00531-015-1226-7

Pupin JP (1980). Zircon and granite petrology. Contribution Mineralogy and Petrology 110: 463–472.

Pupin JP (1988) Granites as indicators in paleogeodynamics. Rendiconti della Società Italiana di Mineralogia e Petrologia 43: 237-262.

Rimmelé G (2003) Structural and Metamorphic Evolution of the Lycian Nappes and the Menderes Massif: Geodynamic Implications with the Aegean Domain. PhD, Institute für Geowissenshaften, Universitat Potsdam, 162 p.

Rimmelé G, Jolivet L, Oberhansli R, Goffe B (2003a). Deformation history of the high-pressure Lycian nappes and implications for tectonic evolution of SW Turkey. Tectonics 22: 1007–1027. https://doi.org/10.1029/2001TC901041

Rimmelé G, Oberhänsli R, Goffé B, Jolivet L, Candan O et al. (2003b). First evidence of high-pressure metamorphism in the "Cover Series" of the southern Menderes Massif. Tectonic and metamorphic implications for the evolution of SW Turkey. Lithos 71: 19-46. http://doi.org/10.1016/S0024-4937(03)00089-6

Robertson AHF, Poisson A, Akıncı Ö (2003). Developments in research concerning Mesozoic-Tertiary Tethys and Neotectonics in the Isparta Angle: SW Turkey. Geological Journal 38: 195-234. https://doi.org/10.1002/gj.953

Sláma J, Košler J, Condon DJ, Crowley JL, Gerdes A et al. (2008). Plešovice zircon-a new natural reference material for U-Pb and Hf isotopic microanalysis. Chemical Geology 249 (1-2): 1-35.

Stacey JS, Kramers JD (1975). Approximation of terrestrial lead isotope evolution by a two-stage model. Earth Planetary Science Letters 26: 207-221. https://doi.org/10.1016/j.chemgeo.2007.11.005

Sun SS, Mcdonough WF (1989). Chemical and isotopic systematics of oceanic basalts; implications for mantle composition and processes. In: Saunders AD, Norry MJ (eds) Magmatism in the Ocean Basins Saunders. Geological Society, London, Special Publication 42: 313-345. https://doi.org/10.1144/gsl.sp.1989.042.01.19

Şengör AMC, Yılmaz Y (1981). Tethyan evolution of Turkey; A plate tectonic approach: Tectonophysics 75: 181-241. https://doi.org/10.1016/0040-1951(81)90275-4

Wiedenbeck M, Allé, Corfu F, Griffin WL, Meier M et al. (1995). Three natural zircon standards for U-Th-Pb, Lu-Hf, trace element and REE analyses. Geostandards Newsletter 19: 1-23. https://doi.org/10.1111/j.1751-908X.1995.tb00147.x

Winchester JA, Floyd PA (1977). Geochemical Discrimination Products Using Immobile Elements. Chemical Geology 20: 325-343. https://doi.org/10.1016/0009-2541(77)90057-2